iScience

CellPress
OPEN ACCESS

Article

Population-specific thermal responses contribute to regional variability in arbovirus transmission with changing climates

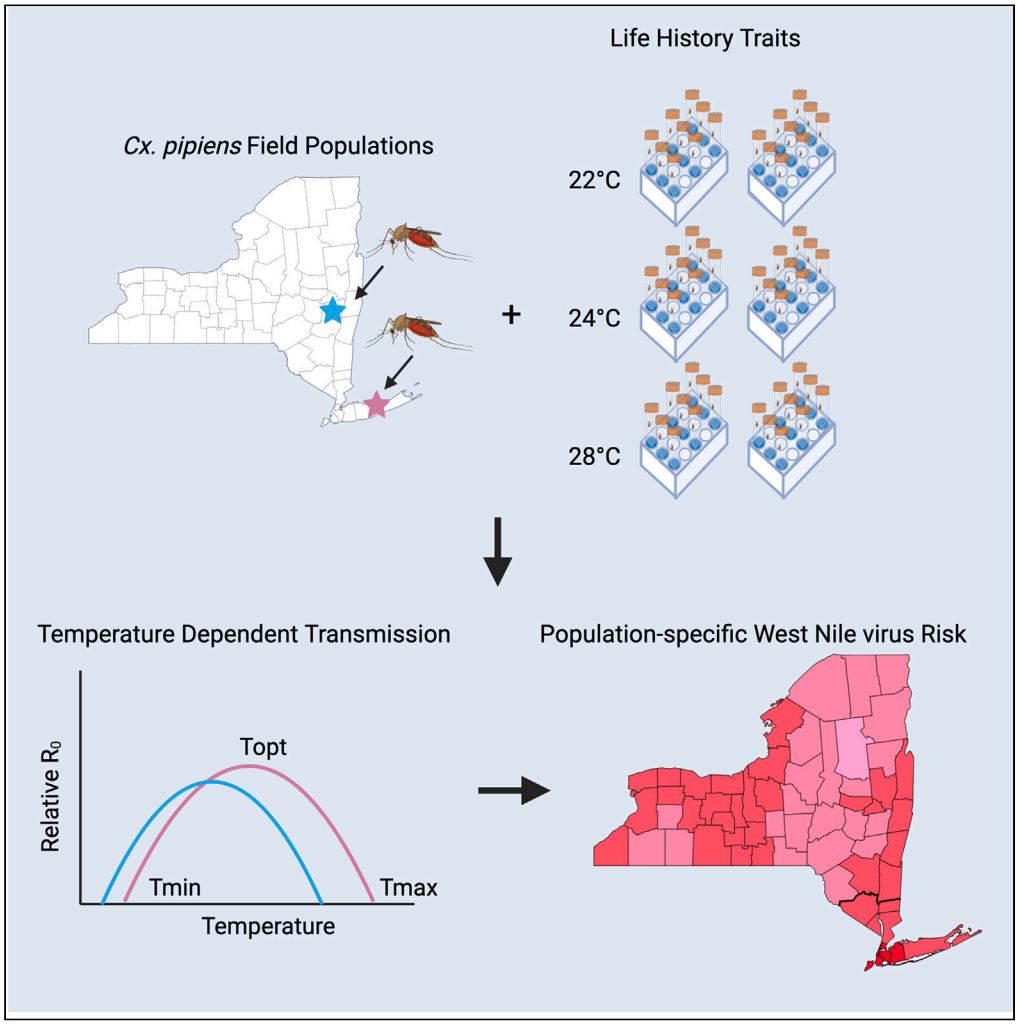

Rachel L. Fay, Mauricio Cruz-Loya, Alexander C. Keyel, Dana C. Price, Steve D. Zink, Erin A. Mordecai, Alexander T. Ciota

alexander.ciota@health.ny.gov

Highlights

Vector-borne pathogens are uniquely susceptible to temperature variation

Variation in Culex life history traits is consistent with local thermal conditions

Population-specific trait-based transmission models reflect pathogen prevalence

Population-specific data can inform more accurate disease models under climate change

Fay et al., iScience 27, 109934
June 21, 2024
https://doi.org/10.1016/j.isci.2024.109934

iScience

CellPress
OPEN ACCESS

Article

Population-specific thermal responses contribute to regional variability in arbovirus transmission with changing climates

Rachel L. Fay,[1,2] Mauricio Cruz-Loya,[3,5] Alexander C. Keyel,[2,5] Dana C. Price,[4] Steve D. Zink,[2] Erin A. Mordecai,[3,6] and Alexander T. Ciota[1,2,6,7,*]

SUMMARY

Temperature is increasing globally, and vector-borne diseases are particularly responsive to such increases. While it is known that temperature influences mosquito life history traits, transmission models have not historically considered population-specific effects of temperature. We assessed the interaction between *Culex pipiens* population and temperature in New York State (NYS) and utilized novel empirical data to inform predictive models of West Nile virus (WNV) transmission. Genetically and regionally distinct populations from NYS were reared at various temperatures, and life history traits were monitored and used to inform trait-based models. Variation in *Cx. pipiens* life history traits and population-dependent thermal responses account for a predicted 2.9°C difference in peak transmission that is reflected in regional differences in WNV prevalence. We additionally identified genetic signatures that may contribute to distinct thermal responses. Together, these data demonstrate how population variation contributes to significant geographic variability in arbovirus transmission with changing climates.

INTRODUCTION

Arthropod-borne viruses are associated with over 140 human diseases. The most geographically widespread arboviruses belong to the *Flaviviridae* family, which includes West Nile virus (WNV), Zika virus, dengue virus (DENV), yellow fever virus, and Japanese encephalitis virus, among others.[1] WNV was first identified in Uganda in 1937 and has a broad global distribution.[2,3] WNV emerged in New York State (NYS) in 1999 and has since spread across the United States (U.S.) and the Americas.[4] WNV is now the most prevalent mosquito-borne virus in the U.S., where it cycles between wild birds and several known vectors, including the primary vector in the Northeast U.S., *Culex pipiens*.[5,6]

Across the globe, average temperatures are increasing.[7] In NYS, temperatures have risen at an average rate of 0.14°C per decade since 1900 and are expected to rise by more than 2.28°C by 2080.[8] This increase will likely significantly alter patterns and intensity of vector-borne disease transmission.[9] Both mosquitoes and the pathogens they transmit are ectotherms, meaning their physiology and life histories are directly influenced by environmental temperature.[10] Temperature-dependent traits drive the biological processes required for transmission.[11] Specifically, temperature has been shown to influence *Culex* spp. blood feeding, fecundity, longevity, development rate, and vector competence.[12–17] Previous studies have demonstrated that while transmissibility of mosquito-borne pathogens is significantly altered by variation in temperature, the magnitude of these effects is species and population specific.[11,12,18–23] Variable temperature sensitivity across mosquito populations could arise in part from genetic variation in thermal responses, which is likely to result in regionally distinct consequences for vector-borne disease transmission under climate change.

Transmission of vector-borne pathogens with changing temperatures has been predicted across the U.S., yet previous studies have utilized generic experimental and surveillance data to model transmission on broad geographical scales without incorporating population-specific differences in thermal sensitivity.[24–27] The goal of this study was to begin to assess the complex interplay between mosquito population and environment in NYS in order to create more accurate regional transmission models of WNV under climate change. Specifically, we address three key questions: (1) Are downstate and upstate NYS populations genetically differentiated, and if so, in which genes and/or metabolic pathways? (2) Do downstate and upstate populations differ in the thermal performance of life history traits, and if so, are these consistent

[1]Department of Biomedical Sciences, State University of New York at Albany School of Public Health, Rensselaer, NY, USA
[2]The Arbovirus Laboratory, Wadsworth Center, New York State Department of Health, Slingerlands, NY, USA
[3]Biology Department, Stanford University, Stanford, CA, USA
[4]Department of Entomology, Rutgers University, New Brunswick, NJ, USA
[5]These authors contributed equally
[6]Senior author
[7]Lead contact
*Correspondence: alexander.ciota@health.ny.gov
https://doi.org/10.1016/j.isci.2024.109934

with local thermal adaptation? (3) How does population-specific life history variation affect the relationship between temperature and pathogen transmission, and do field data support these predictions?

To address these questions, we first conducted population genetic analyses on two field acquired populations of *Cx. pipiens* from downstate and upstate NYS. Then, we experimentally measured life history traits at regionally relevant current and future transmission temperatures of 22°C, 25°C, and 28°C. Using thermal performance curves fit to these data, we modeled the basic reproduction number (R_0) of WNV across temperatures and validated this model by comparing it with field data of regional mosquito infection rates in NYS. Together, the results demonstrate that the effect of temperature is population dependent and consistent with local adaptation and that this variability will likely contribute to regional differences in transmissibility under climate change.

RESULTS

Genotyping of distinct populations of *Culex pipiens*

Pool-seq analysis using 299.8M and 302.0M Illumina HiSeq paired-end reads generated for respective downstate and upstate *Cx. pipiens* populations identified 10,432,033 polymorphic sites between the two populations, of which 4,110,691 were significant ($p < 0.05$) after Fisher's exact test calculation. Using the genome annotation, we identified 1,154,833 significant SNPs (single nucleotide polymorphisms) within the 109.3 Mbp of gene coding sequence (Table S1). Using the 95th percentile of genes ranked by most SNPs per bp, we find 14 statistically enriched gene ontology terms among the three major divisions (6 [molecular function], 3 [cellular component], and 5 [biological process]; Figure 1). These could be condensed into the major parent lineages/processes: exopeptidase, fibroblast growth factor, odorant binding, alkane 1-monooxygenase (molecular function), sensory perception, post-embryonic development, response to bacterium (biological process), and extracellular space, intraciliary transport, and dendrite membrane (cellular compartment). Notably, we identified multiple cytochrome P450 (CYP) enzymes within GO:0016713 (alkane 1-monooxygenase activity)/GO:0042742 (response to bacterium) as well as dipeptidyl peptidases (GO:0008239) in this enriched set, discussed in the further texts.

Cx. pipiens sensu stricto consists of two biotypes that overlap throughout North America: form pipiens and form molestus, each with varying behavioral and physiological differences.[30,31] To assess the degree of ancestry from either form in our data, we examined sequencing reads derived from the diagnostic CQ11 locus which has been shown to differentiate both forms[32] and find that ca. 38.7–47.0% of pooled Suffolk *Cx. pipiens* mosquitoes encode a *Cx. pipiens* form molestus type allele, while ca. 10.3–11.5% of Albany mosquitoes encode the same (Figure S2; estimates made from two positions in alignment).

Immature development and survival

In order to quantify the extent of population-dependent variability in physiological responses to temperature, life history traits of the two genetically distinct field populations of *Cx. pipiens* from NYS were evaluated at 22°C, 25°C, and 28°C under controlled conditions in the laboratory.

Larval survival was significantly higher for the downstate *Cx. pipiens* compared to the upstate *Cx. pipiens* at both low and high temperatures (97% vs. 87% at 22°C and 96% vs. 41% at 28°C; Figure 2A; Chi-squared test, $p < 0.05$), while survival was similar at the intermediate temperature (88–89% at 25°C). Using these data, we refine previous estimates[11] of species-wide thermal performance curves (TPCs) of six *Cx. pipiens* life history traits (adult lifespan, development rate, larval survival to adulthood, blood feeding, proportion ovipositing, and number of eggs per raft) to population-specific TPCs for the upstate and downstate populations with a Bayesian approach. With these population-specific TPCs, we obtain estimates of the temperature dependence of R_0 for the upstate and downstate populations (see STAR Methods and Appendix for details, code is available in GitHub) with the main goal of comparing the optimal transmission temperature for WNV in these populations. The measured temperature range for the life history traits in the NYS populations (22°C–28°C) encompasses the range of temperatures where the transmission temperature optimum is likely to be in (previous studies in *Cx. pipiens* place this optimum around 24.5°C).[11] This makes it possible to estimate population-specific thermal optima for R_0 based on the data for the individual traits. However, estimates of minimum and maximum temperatures are largely based on previous estimates in other *Cx. pipiens* populations. Because of this, they should be interpreted with caution, especially when the estimated values are far from the temperature range where measurements are available.

Our thermal performance curve analysis demonstrates that the downstate population has a higher temperature maximum (40.4°C, 95% CI:[37.9, 43.3]) and optimum (23.9°C, 95%CI:[22.1, 25.8]) for larval survival compared to that of the upstate population, which had a maximum of 32.9°C, 95%CI:[31.4, 34.8] and an optimum of 19.4°C 95%CI:[17.7, 21.1] (Figure 2B; Table 1). Importantly, the credible intervals do not overlap, demonstrating substantial differences between the larval survival of the upstate and downstate populations, consistent with local thermal adaptation. In contrast to the optimum and maximum temperatures, our analysis did not detect a clear difference between temperature minima for larval survival, which were estimated to be 7.4°C, 95%CI:[4.2, 10.3] for the downstate and 6.0°C, 95%CI:[2.7, 9.1] for the upstate populations.

In general, as temperature increases, mosquito development rate is accelerated (Figure 2C). At both 22°C and 25°C the upstate population demonstrated shorter development time compared to the downstate population, but this difference was not statistically significant ($p > 0.05$). Thermal performance curves demonstrate an accelerated development rate for the upstate population across temperatures up to ~30.0°C. The fitted thermal performance curves depict a range of 2.4°C, 95%CI:[-1.1, 5.6] to 37.0°C, 95%CI:[34.8, 39.5] for the upstate population, and 6.3°C, 95%CI:[3.3, 8.8] to 40.3°C, 95%CI:[37.9, 42.7] for the downstate population. The estimated optimum temperature for mosquito development was ~3°C higher in the downstate population, although our analysis is not conclusive about this possible difference due to

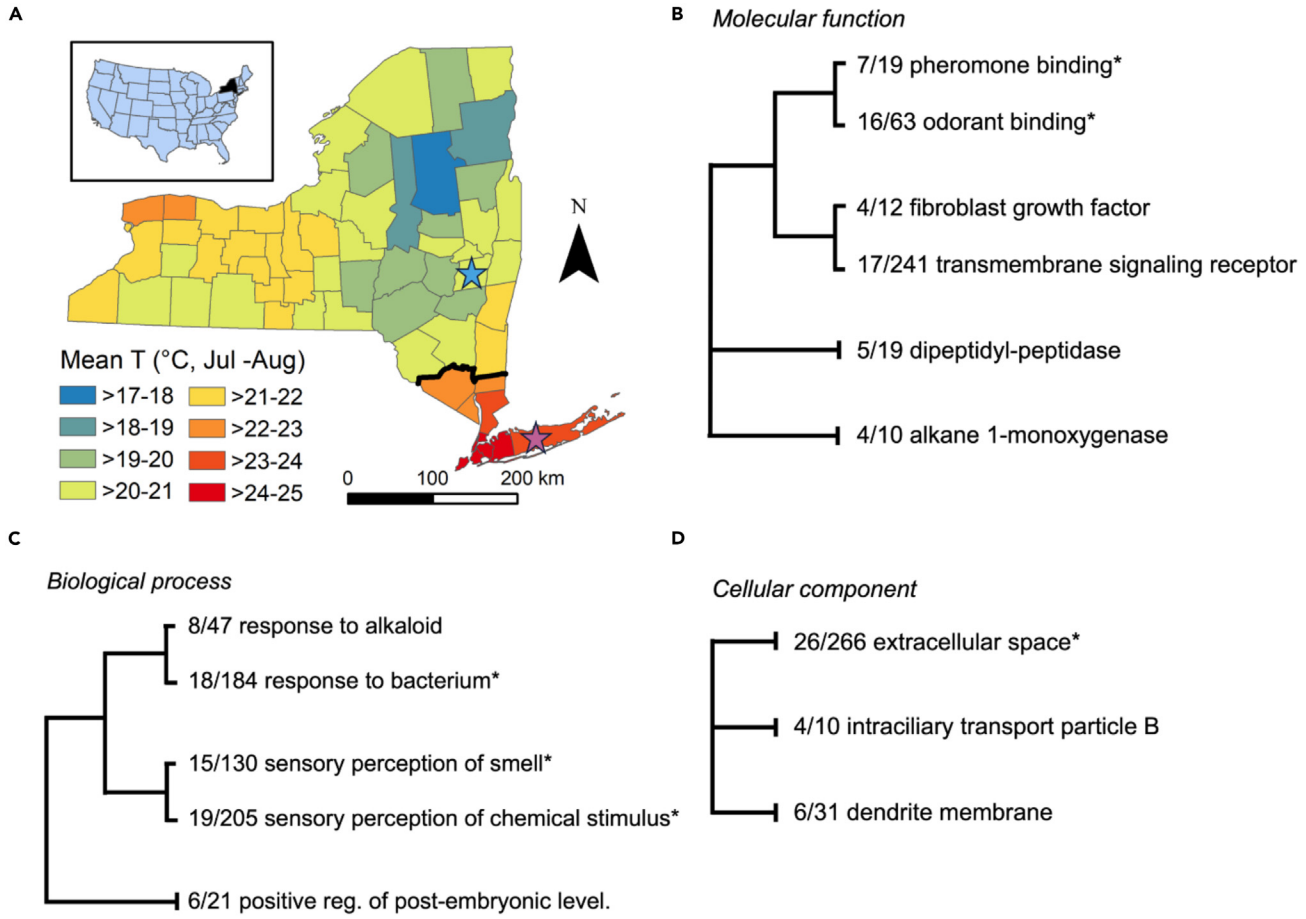

Figure 1. County-level average temperature during peak West Nile virus transmission season and genetic characterization of *Culex pipiens* from climactically distinct regions of New York State

(A) The county level average temperatures (C°) for July and August 2021 are depicted by shading. Temperature data utilized were derived from GRIDmet, Abatzoglou, 2013.[28,29] *Culex pipiens* were acquired from two counties in New York, the blue star indicating Albany County and the pink star indicating Suffolk County. The black line depicts the designation of upstate and downstate counties based on distinct temperature profiles. The inset shows the location of NYS (black) in the US.

(B–D) Enrichment of gene ontology (GO) terms assigned to the 95th percentile (top 5%) of genes ranked by descending significant single nucleotide polymorphisms per base pair of gene length in the *Cx. pipiens* upstate vs. downstate population comparison. Numbers indicate terms in the test set/reference set. Asterisks indicate terms enriched with adjusted *p*-value of 0.01; remainder at 0.05. Further details regarding GO term enrichment and constituent genes given in Table S2. Clustering of GO terms is based on shared members.

the uncertainty in the estimates (29.9°C, 95%CI:[28.4, 31.6] vs 32.9°C, 95%CI:[31.2, 34.8]; Figure 2D; Table 1). Both temperature and population have a significant effect on mosquito development rate (Figure 2C; two-way ANOVA, $p < 0.05$). Average wing length was used to assess the relationship between temperature and body size, and both temperature and population were found to have a significant effect on wing length (Figure S1; two-way ANOVA, $p < 0.05$). Specifically, body size was on average higher for the upstate population and, consistent with accelerated development, increased temperature was associated with decreased body size.

Adult survival

Temperature had a significant effect on adult longevity, with decreased mean survival associated with increased temperature (Figures 3A–3E; two-way ANOVA $p < 0.05$), yet neither population nor the interaction between population and temperature had a significant effect (Figure 3D; two-way ANOVA, $p > 0.05$). The highest mean survival was measured at 22°C for the upstate population (25.0 days) and at 25°C for the downstate population (24.0 days), a trend that is consistent with local thermal adaptation. Adult female mosquitoes in the upstate and downstate populations have similar lifespans across temperatures, with the estimated maximum survival temperature being 37.2°C, 95%CI:[34.4, 40.5] for the downstate population and 35.8°C, 95%CI:[33.1, 39.2] for the upstate population (Figure 3E; Table 1).

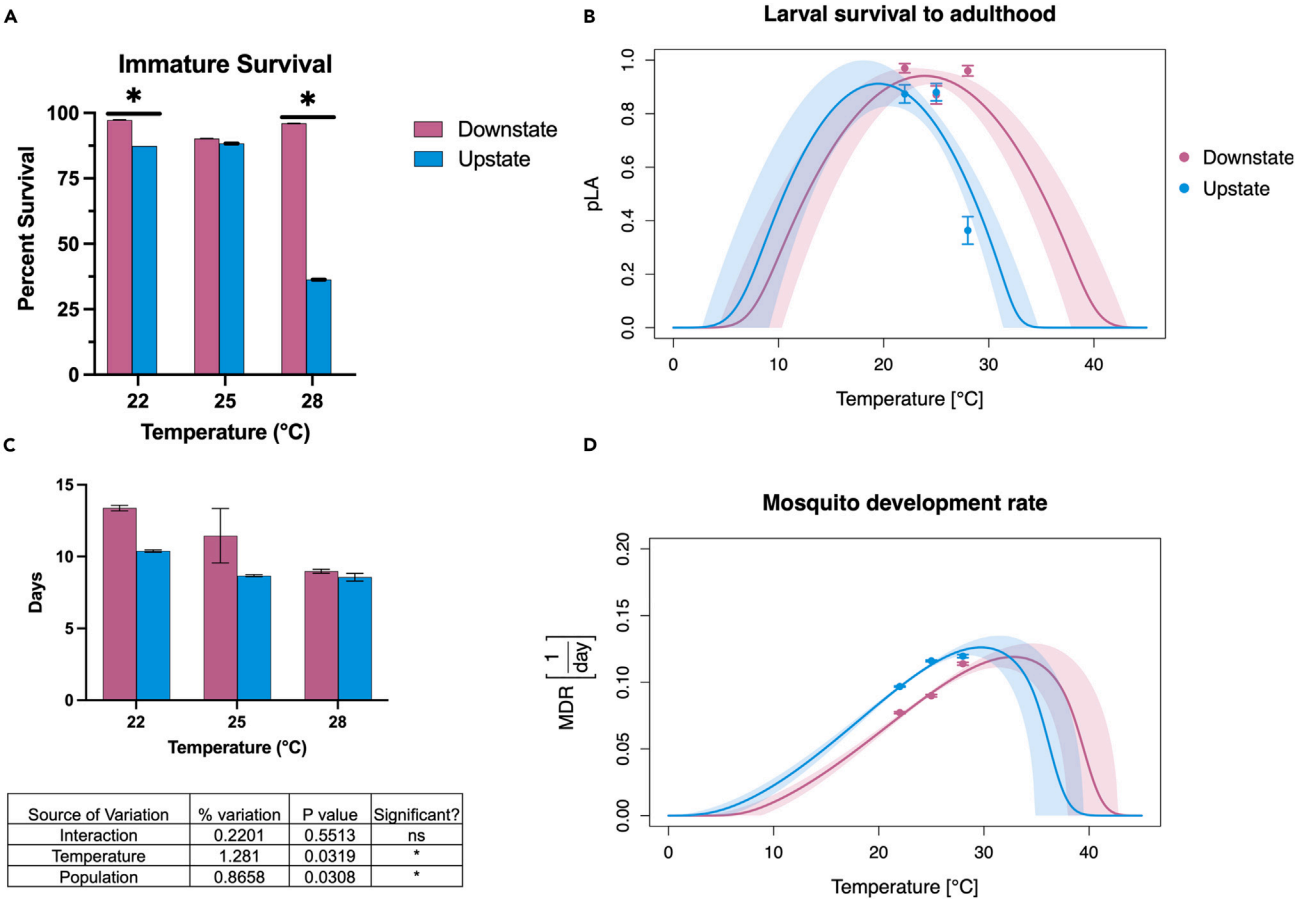

Source of Variation	% variation	P value	Significant?
Interaction	0.2201	0.5513	ns
Temperature	1.281	0.0319	*
Population	0.8658	0.0308	*

Figure 2. Immature survival and development differ between populations of *Culex pipiens* from downstate and upstate New York State

(A) Percent of larvae surviving to adulthood +/− SEM.

(B) Thermal performance curve for larval-to-adult survival (pLA). Points represent survival proportions at each temperature with standard error. Lines represent the posterior mean, and shaded regions 95% credible intervals (CIs) of a quadratic model fit.

(C) Development time in mean days to emergence +/− SEM.

(D) Thermal performance curve for mosquito development rate (MDR). Points represent mean MDR at each temperature with standard error. Lines represent the posterior mean, and shaded regions depict 95% credible intervals (CIs) of a Briere model fit. *$p \leq 0.05$ (chi-squared test or two-way ANOVA w/multiple comparisons, Tukey's post-test).

Blood feeding and fecundity

Significant differences were found in blood feeding and ovipositing between populations at each temperature (Figures 4A and 4C; Chi-squared test, $p < 0.05$). Specifically, the proportion of individuals blood feeding, and subsequently ovipositing, was significantly higher for the downstate population at both 25°C and 28°C, and for the upstate population at 22°C (Figures 4A and 4C; Chi-squared test, $p < 0.05$), again consistent with local thermal adaptation. These differences resulted in thermal performance curves for blood feeding between populations with different profiles (Figure 4B; Table 1). The estimates for the thermal maximum of the populations (upstate = 38.4°C, 95%CI:[34.2, 42.5] v. downstate = 39.4°C, 95%CI:[35.4, 43.4]) were similar between the populations. While the estimates for both the thermal minimum (7.3°C, 95%CI:[0.4, 13.4] v 16.4°C, 95%CI:[8.6, 20.2]) and optimum (22.8°C, 95%CI:[18.9, 26.5] v 27.9°C, 95%CI:[24.1, 30.6]) were more than 5°C higher for the downstate population. These data suggest differences in the thermal minimum and optimum for blood feeding in these populations, yet our analyses are inconclusive about these differences due to the overlapping credible intervals (Figure 4B; Table 1).

Consistent with blood feeding differences, the downstate population had increased ovipositing at higher temperatures compared to the upstate population. The critical thermal minimum and maximum from the fitted thermal performance curve were 7.7°C, 95%CI:[2.0, 13.0] and 30.4°C, 95%CI:[28.2, 35.3] for the upstate population, and 10.1°C, 95%CI:[3.7, 16.6] and 34.2°C, 95%CI:[30.5, 38.9] for the downstate population. Although the point estimates differ by approximately 3°C, when considering parameter uncertainty, we again do not find a substantial difference between the thermal optimum of the upstate and downstate populations based on overlapping credible intervals (19.0°C, 95% CI:[15.8, 22.4] v 22.1°C, 95%CI:[18.6, 25.6]; Figure 3D; Table 1).

Table 1. Thermal response functions and parameter estimates for each trait and population

Trait/Population	F(x)	Parameter	Mean (°C)	2.5%	97.5%
pLA					
Downstate	Q	Tmin	7.4	4.2	10.3
		Tmax	40.4	37.9	43.3
		Topt	23.9	22.1	25.8
Upstate	Q	Tmin	6.0	2.7	9.1
		Tmax	32.9	31.4	34.8
		Topt	19.4	17.7	21.1
MDR					
Downstate	B	Tmin	6.3	3.3	8.8
		Tmax	40.3	37.9	42.7
		Topt	32.9	31.2	34.8
Upstate	B	Tmin	2.4	−1.1	5.6
		Tmax	37.0	34.8	39.5
		Topt	29.9	28.4	31.6
Lifespan					
Downstate	L	m	1.8	1.4	2.4
		Tmax	37.2	34.4	40.5
Upstate	L	m	1.9	1.4	2.5
		Tmax	35.8	33.1	39.2
a					
Downstate	Q	Tmin	16.4	8.6	20.2
		Tmax	39.4	35.4	43.4
		Topt	27.9	24.1	30.6
Upstate	Q	Tmin	7.3	0.4	13.4
		Tmax	38.4	34.2	42.5
		Topt	22.8	18.9	26.5
pO					
Downstate	Q	Tmin	10.1	3.7	16.6
		Tmax	34.2	30.5	38.9
		Topt	22.1	18.6	25.6
Upstate	Q	Tmin	7.7	2.0	13.0
		Tmax	30.4	28.2	35.3
		Topt	19.0	15.8	22.4
ER					
Downstate	Q	Tmin	5.9	1.2	10.4
		Tmax	38.8	35.0	43.0
		Topt	22.4	19.2	25.6
Upstate	Q	Tmin	5.5	0.9	9.9
		Tmax	39.0	34.8	43.5
		Topt	22.3	18.9	25.6

Thermal responses were fit with either a Briere function (B): $B(T) = cT(T - T_{min})(T_{max} - T)^{1/2}$; a quadratic function (Q): $(T) = c(T - T_{min})(T_{max} - T)$, or a linear fit (L): $L(T) = m(T_{max} - T)$. Parameters are reported as the posterior mean and 2.5% and 97.5% quantiles, corresponding to a 95% credible interval. Temperatures are reported in units of degrees Celsius (°C). For the linear fits to lifespan, the slope m is reported in units of days/°C. A more comprehensive summary of the posterior distribution of all model parameters is included in the Appendix.

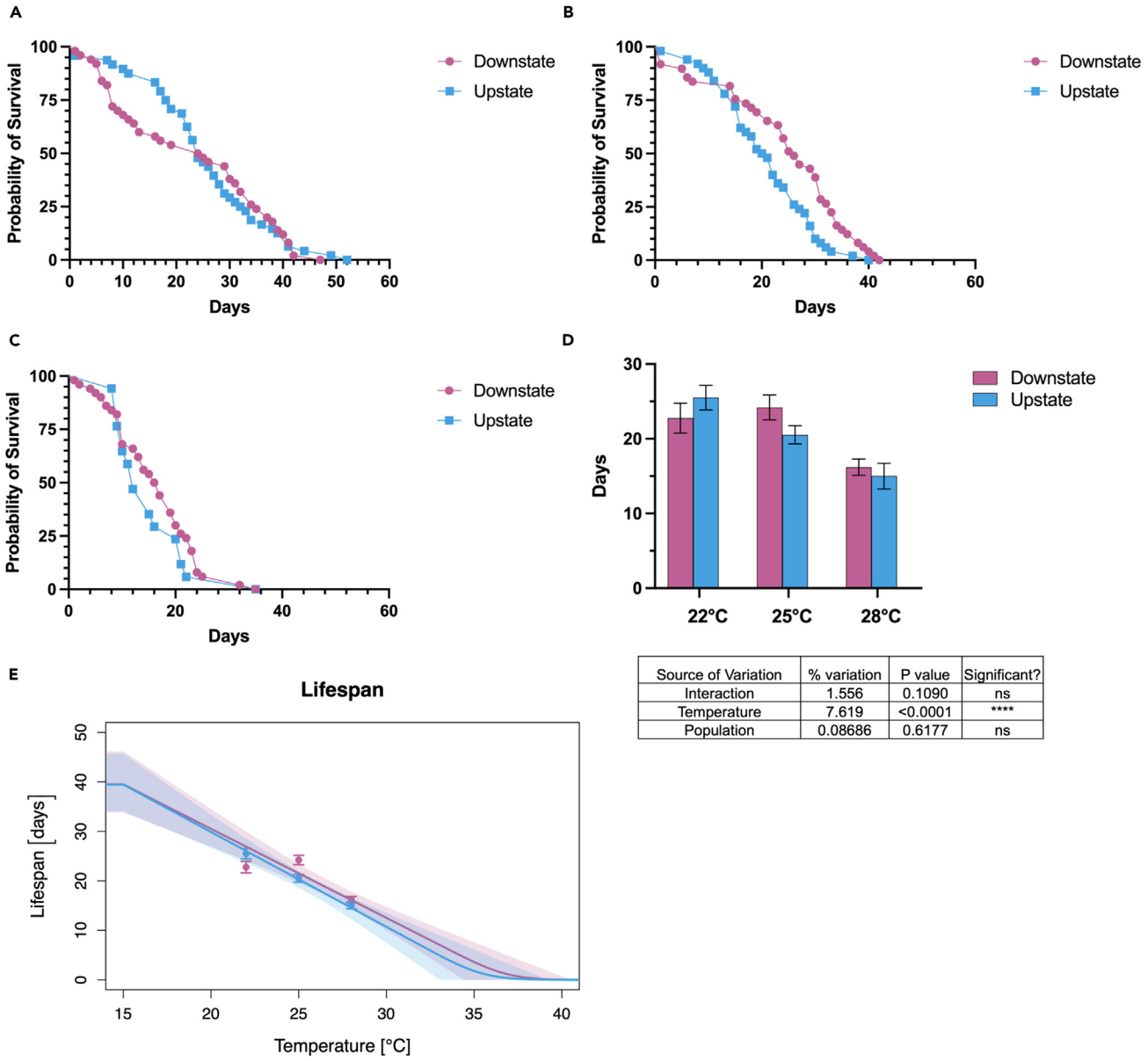

Source of Variation	% variation	P value	Significant?
Interaction	1.556	0.1090	ns
Temperature	7.619	<0.0001	****
Population	0.08686	0.6177	ns

Figure 3. Temperature-dependent adult survival of *Culex pipiens* from downstate and upstate New York State

(A) Probability of daily adult survival at 22°C.

(B) Probability of daily survival at 25°C.

(C) Probability of daily survival at 28°C.

(D) Mean adult longevity +/− SEM.

(E) Thermal performance curve for lifespan (lf). Points represent mean lifespan at each temperature with standard error. Lines represent the posterior mean, and shaded regions depict 95% credible intervals (CIs) of a linear model fit. *$p \leq 0.05$ (two-way ANOVA w/multiple comparisons, Tukey's post-test or log-rank test).

While an increased mean number of eggs per raft was measured for the upstate population at all temperatures compared to the downstate population, this trend was not statistically significant (Figures 4E and 4F; t test, $p > 0.05$). The critical thermal minimum and maximum from the fitted thermal performance curves were very similar between the populations, estimated to be 5.5°C, 95% CI:[0.9, 9.9] and 39.0°C, 95%CI:[34.8, 43.5] for the upstate population, and 5.9°C, 95%CI:[1.2, 10.4] and 38.8°C, 95%CI:[35.0, 43.0] for the downstate population. The optimum temperature estimates were also very similar (22.3°C, 95%CI:[18.9, 25.6] vs 22.4°C, 95% CI:[19.2, 25.6]; Figure 4F; Table 1), demonstrating no significant difference in egg raft size across temperatures between these populations.

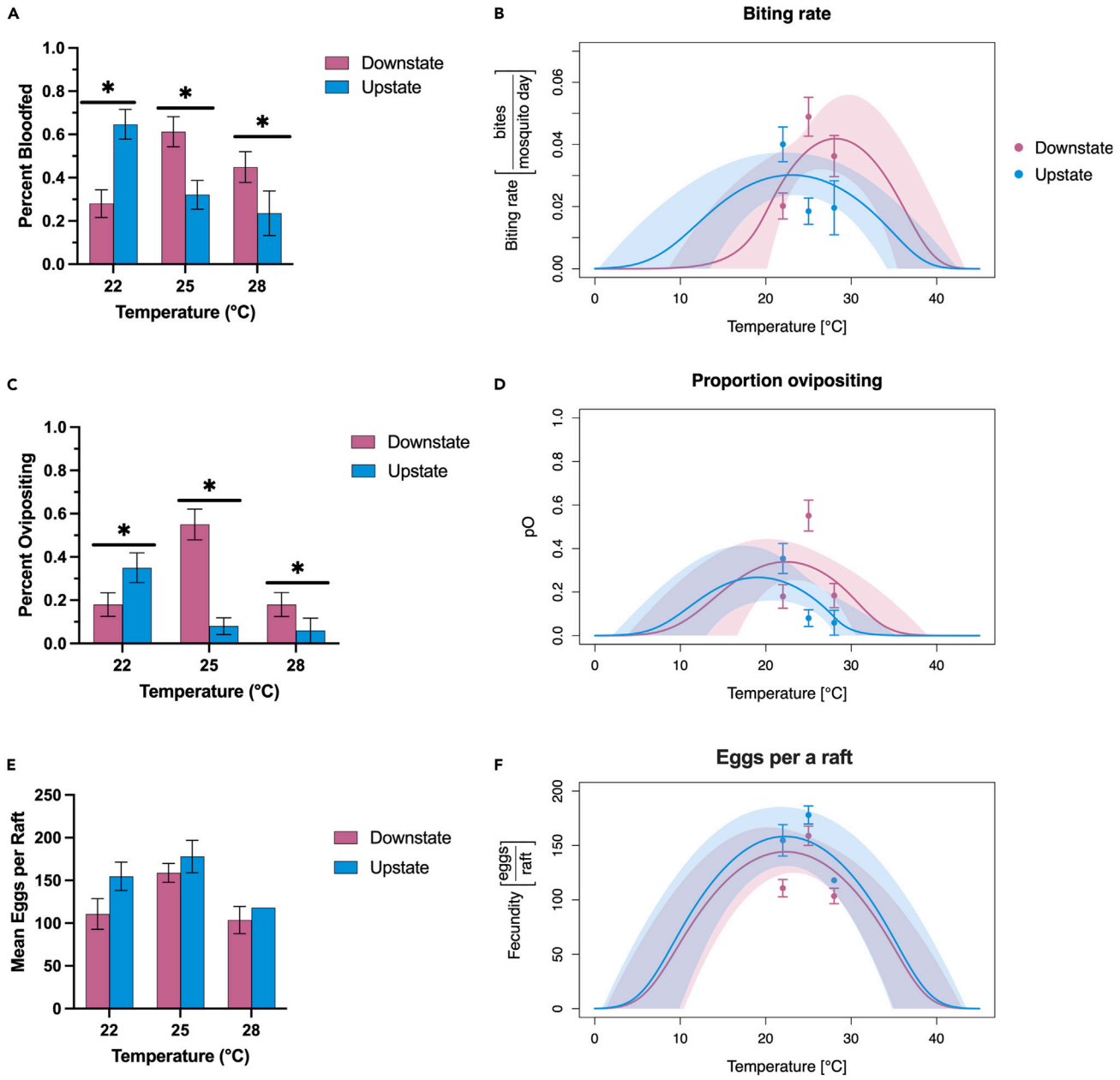

Figure 4. Temperature and population-specific blood feeding and fecundity of *Culex pipiens* from New York State

(A) Percent of blood fed *Culex pipiens* at various temperatures +/− SEM.

(B) Thermal performance curve for biting rate. Points represent proportion of days for which mosquitoes fed during their lifetime at each temperature, with error bars representing standard error. Lines represent the posterior mean, and shaded regions depict 95% confidence intervals [CIs] of a quadratic model fit.

(C) Percent ovipositing +/− SEM.

(D) Thermal performance curve for percent ovipositing (pO). Points represent ovipositing proportions at each temperature, with error bars corresponding to standard error. Lines represent the posterior mean, and shaded regions 95% CIs of a quadratic model fit.

(E) Mean number of eggs per raft +/− SEM.

(F) Thermal performance curve for fecundity (eggs per raft: ER). Points represent the mean number of eggs per raft at each temperature, with error bars corresponding to standard error. Lines represent the posterior mean, and shaded regions depict 95% credible intervals (CIs) of a quadratic model fit. *$p \leq 0.05$ (chi-squared test).

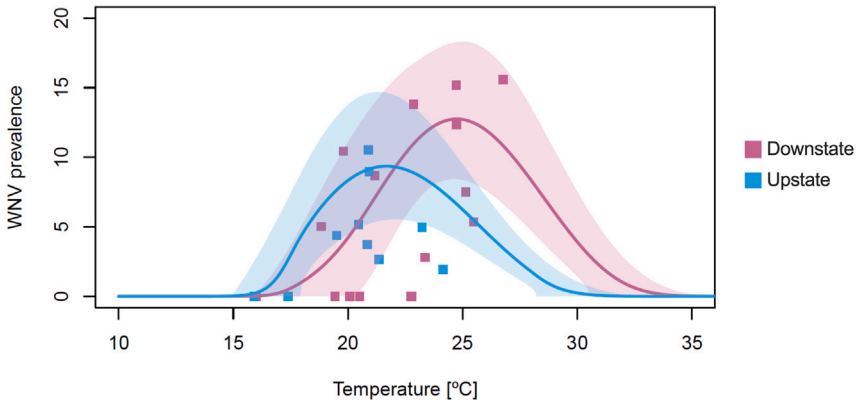

Figure 5. Population-specific transmissibility of West Nile virus by *Culex pipiens* is consistent with regional thermal adaptation and pathogen prevalence

Lines represent posterior mean estimates, and shaded regions 95% credible intervals, of the estimated relative R_0 for the upstate and downstate *Culex pipiens* populations. Relative R_0 estimates were calculated using the thermal performance curves shown in Figures 3, 4, and 5, including larval-to-adult survival (pLA), adult lifespan (lf), mosquito development rate (MDR), biting rate (a), percent ovipositing (pO), and eggs per raft (ER). All other traits were calculated using thermal performance curves from Shocket et al. WNV prevalence, shown as squares, represents weekly maximum likelihood estimates of the number of virus positive *Culex* spp. per 1,000 tested by region during the 2022 transmission season plotted against the mean weekly temperature two weeks before collection. Relative R_0 is shown scaled to approximately match the range of the WNV prevalence data. WNV prevalence and relative R_0 exhibit similar regional variability thermal relationships.

Predicted R_0

To understand how population differences in thermal performance of multiple life history traits translate into differences in transmission potential across temperatures, we calculated temperature-dependent relative R_0 using a previously published model by Shocket et al. 2020.[11] Additional thermal performance curves of traits necessary to calculate relative R_0 not recorded in this study (pathogen development rate, vector competence and egg viability) were taken from species-wide TPCs for *Cx. pipiens* estimated in this previous work (based on previously published code).[11] For both populations there is a unimodal relationship between relative R_0 and temperature, as expected from previous work.[11,23] Importantly, the upstate and downstate populations differed in the optimal temperature for relative R_0, which corresponds to the predicted temperature of peak transmission of WNV in these populations (Figure 5; Table 2). Consistent with thermal adaptation, the predicted peak temperature for WNV transmission in upstate *Cx. pipiens* was substantially lower than for the downstate population (21.7°C, 95%CI:[20.7, 22.8] versus 24.6°C, 95%CI:[22.9, 26.0], respectively), with an estimated difference of 2.9°C, and a >95% posterior probability that the difference is greater than 1°C (see Appendix). In contrast, the estimated thermal minima did not differ substantially between the populations (16.8°C, 95%CI:[15.0, 17.9] v 17.8°C, 95%CI:[15.7, 20.2]). The point estimate for the thermal maximum for WNV transmission was approximately 3.7°C lower for the upstate than the downstate population (30.2°C, 95%CI:[28.2, 33.3] v 33.9°C, 95%CI:[30.5, 37.2]). However, since the credible intervals for the temperature maxima were wider compared to those for temperature optima, our analysis is inconclusive about population-specific differences between the maximum temperature for relative R_0. The fitted thermal performance curves also predict the downstate population to have a wider thermal range for WNV transmission compared to the upstate population (~16°C vs. 13°C).

Mosquito surveillance and temperature

We validated the model predictions, which are based on laboratory experimental data, using field data from *Culex* mosquitoes collected in upstate (Erie County) and downstate (Suffolk County) from 7/17/22 to 10/8/22. We detected WNV infection in 30 of 196 pools consisting of 7,065 individual *Culex* mosquitoes from upstate and in 94 of 449 pools consisting of 15,205 individuals from downstate. Weekly prevalence (WNV positive/1000) was estimated based on pool size and compared to mean weekly temperatures in each county at the time of collection (Figure 5), resulting in ranges of prevalence and temperature (upstate: prevalence 0–13.8 (week of 8/28), mean 4.4, and temperature 10.2°C–24.1°C; downstate prevalence 0–13.1 (week of 8/28), mean 7.9, and temperature 13.6°C–26.8°C). While there is significant variability and there is no standard nonlinear model which fully describes the relationships between prevalence and temperature, local prevalence data support regional adaptation largely consistent with our population-specific R_0 models (Figure 5). Additionally, Spearman's correlation was computed to assess the relationship between relative R_0 and WNV prevalence in mosquitoes. There was a positive correlation between the two variables for each population: downstate (0.454, 95%CI:[0.094, 0.568]) and upstate (0.623, 95%CI [0.354, 0.790]).

Risk in New York State

County level temperature suitability predictions for WNV transmission in NYS were inferred using region-specific R_0 models under 1, 2, or 3°C increases in average temperatures. Statewide risk is generally predicted to be higher compared to present day risk during historic peak season (July and August) with a 1°C increase (Figures 6A, 6B, and S4). With 2°C of warming, regional variability in temperature and mosquito

Table 2. Estimated thermal limits and optima for relative R_0 in *Culex pipiens* populations from New York State

Population	Parameter	Mean (°C)	2.5% (°C)	97.5% (°C)
Downstate	Tmin	17.8	15.6	20.2
	Tmax	33.9	30.6	37.2
	Topt	24.6	22.9	26.0
Upstate	Tmin	16.7	15.0	17.9
	Tmax	30.2	28.2	33.3
	Topt	21.7	20.7	22.8

For each population, we report the posterior mean and 2.5% and 97.5% quantiles, representing a 95% credible interval of the minimum (Tmin), maximum (Tmax) and optimum/peak transmission (Topt) temperatures for relative R_0.

population result in increased heterogeneity in predicted risk. In this scenario, a continued increase in transmission is predicted for downstate counties as well as Central and Northern NYS, yet predicted risk decreases in Western and Eastern NYS. Further decreases are predicted statewide with 3°C of warming, with the exception of Central and Northern NYS. Importantly, decreased risk in July and August could to

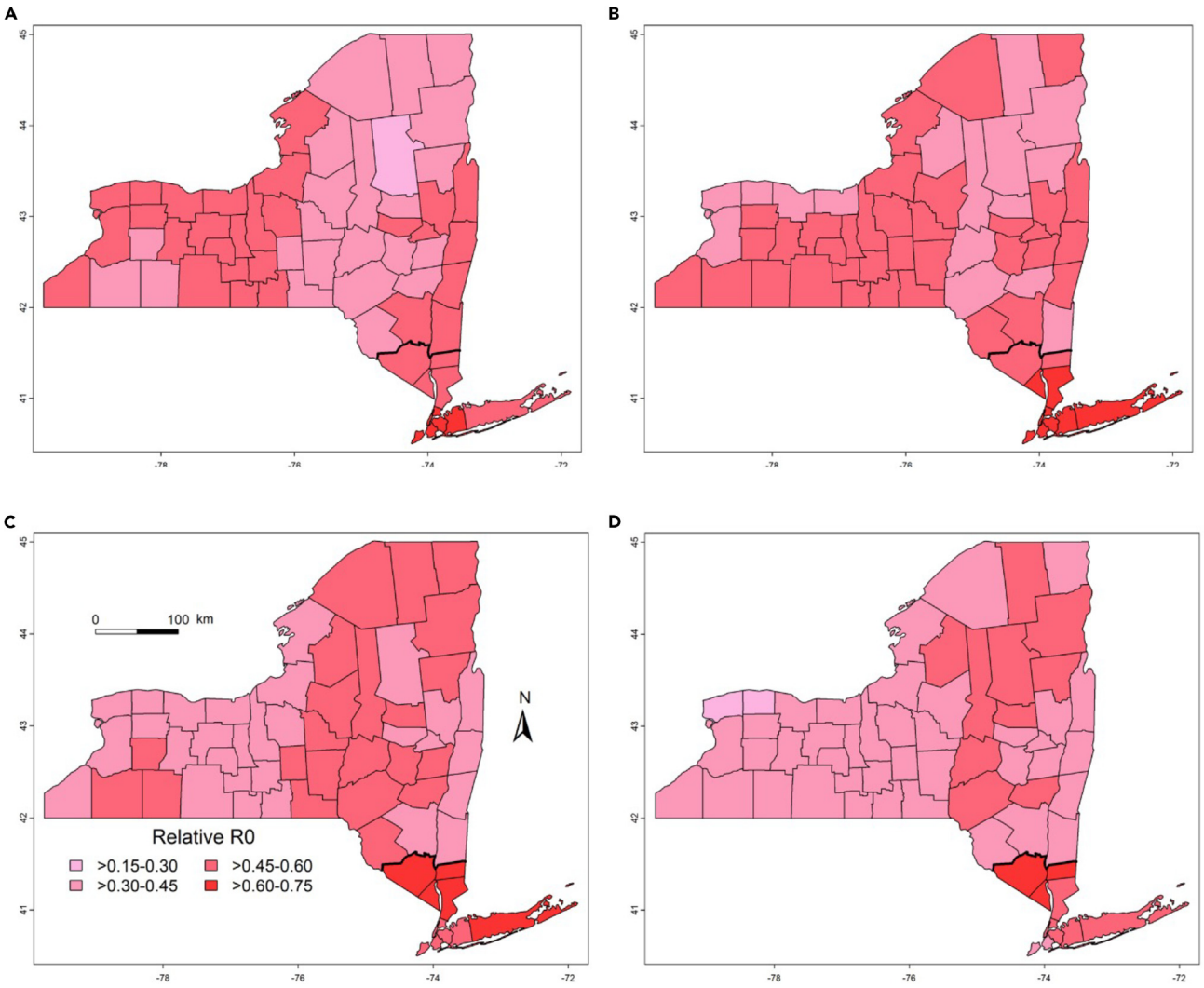

Figure 6. Relative R_0 by county, using R_0 values for Albany for upstate counties and R_0 values for Suffolk for downstate counties

(A) County-level mean present day risk, while series shows the change in the median R_0 for (B) 1°C, (C) 2°C, (D) 3°C of warming. Black line indicates the boundary between upstate and downstate counties. Temperature inputs for R_0 correspond to mean July/August temperatures for 2021.

some extent be offset by increased risk in cooler months, and climate change scenarios based on the CMIP6 model show June and September becoming increasingly important in annual WNV risk across NYS (Figure S3).

DISCUSSION

Climate change is expected to substantially affect transmission of vector-borne pathogens including WNV, yet trait-based models aiming to predict climate-driven changes in vector-borne disease transmission have historically lacked information on regional variation and local thermal adaptation.[11,25,33–36] Here, we provide evidence of local variability in thermal performance consistent with regional adaptation in vector mosquitoes (Figures 2, 3, 4, 5, and 6) from genetically distinct populations (Figure 1), and we demonstrate that effects of experimentally measured thermal adaptation in life history traits can broadly predict patterns of transmission in the wild (Figure 6). We utilized previously published data to fill in gaps at the minimum and maximum temperatures for life history traits recorded in this study, as well as thermal performance curves unique to both *Culex pipiens* and WNV for traits not investigated during this study.[11] Specifically, we demonstrate that representative populations of *Cx. pipiens* from distinct regions in NYS (Figure 1) are both genetically divergent (Figure 1) and unique in temperature sensitivity profiles for immature survival and development rate (Figure 2), adult longevity (Figure 3), blood feeding (Figure 4) and fecundity (Figure 4). These differences result in a predicted 2.9°C difference in peak WNV transmission temperature between upstate and downstate *Cx. pipiens* based on trait-based R_0 models: a prediction that was validated by field surveillance data considering weekly WNV prevalence in *Culex* spp. mosquitoes and temperature. Together, these data demonstrate the profound effect regional variability in thermal responses can have on arbovirus transmission risk with changing climates.

Previous studies have utilized experimental data from variable field and colony mosquito populations to estimate species-level relationships between temperature, mosquito life-history traits, and virus transmission for WNV.[11,37] Shocket et al. (2020) determined the optimal temperature for WNV transmission by *Cx. pipiens* to be 24.5°C and demonstrated important species-specific variability in thermal performance across *Culex* vectors.[11] Our estimates for the downstate population largely agree with the previous model (with a predicted optimum of 24.6°C), but optimal transmission temperatures were found to be significantly lower (21.7°C) for the upstate population. While we also found population variability in thermal minima and maxima, our experimental temperature range of 22°C–28°C limited the capacity to accurately estimate population-specific extremes. In particular, minimum temperature estimates for life history traits are extrapolations outside of the range of the empirical data, so true trait minimums may lie beyond the credible intervals estimated by the models. However, this does not affect the population R_0 estimates here, as vector competence limits the lower bound of R_0.[11] Identifying population-specific thermal minima and maxima should be a focus of future studies. An additional limitation of these models is that in nature mosquitoes experience diurnal temperature cycles, whereas our experiments and models focused on constant temperatures. Integrating the models across realistic daily and seasonal temperature regimes could refine predictions under varying temperatures, and previous studies suggest that such approaches are generally accurate, although variability in immature development time and fecundity may exist.[38,39]

The most important drivers of variation in thermal responses between populations were immature survival and the proportion of mosquitoes blood feeding and ovipositing, although the population thermal responses also varied for mosquito development rate. In every case, the downstate population performed better at warmer temperatures, providing strong evidence for local thermal adaptation. Population-specific differences are well documented, but the existence of local thermal adaption in mosquito populations has yet to be investigated in the context of pathogen transmission models.[15,40–44]

Population differences in the proportional ancestry of *Cx. pipiens* molestus could contribute to differences in thermal performance. *Cx. pipiens* molestus is a bioform of *Cx. pipiens* which is morphologically similar to *Cx. pipiens* pipiens but differs in behavioral and physiological signatures. We identified *Cx. pipiens* molestus genetic signatures in both the downstate and upstate populations, but the downstate population had a higher proportion of molestus ancestry. *Cx. pipiens* molestus occupy subterranean habits, more frequently feed on mammals, and are both autogenous and stenogamous.[45] These ecological and physiological differences could contribute to differences in thermal adaptation. To our knowledge, genetic factors responsible for thermal adaptation at the population level in mosquitoes are largely unknown.

Examination of enriched gene ontology (GO) terms yields several candidates for further consideration; among these are the prolylcarboxypeptidases (PRCPs) that together compose the dipeptidylpeptidase activity ontology (GO:0008239; Table S2). PRCP activity is positively correlated with several metabolic parameters in vertebrates including mice and humans[46] and has been shown to regulate cell growth, vascular repair, and is linked to a function in the digestive tract of insects.[43]

A second gene family enriched in the test set comprises several cytochrome P450 enzymes assigned to the alkane 1-monooxygenase activity ontology (GO:0016713; Table S2). Although CyP450s are generally associated with detoxification and breakdown of insecticidal compounds, enzymes in the CYP6 family additionally play essential roles in hormone synthesis, including juvenile hormone,[47] as well as thermal adaptation and diapause in flies.[48,49]

It is also possible that only one or few genes may cf. the phenotype(s) measured here and thus may be overlooked when analyses are conducted at the level of gene ontology. Of the 834 genes present in the 95th percentile of our ranked dataset, 123 (14.7%) were reported as differentially expressed genes upon exposure of *Cx. pipiens pallens* to low-temperature stress.[50] Within these 123 genes are two heat shock protein members, HSP70 and HSP20. Heat shock proteins (HSPs) comprise gene clusters that are commonly associated with lineage and species-specific mosquito thermal response.[51] We manually identified two HSPs in the 95th percentile of our ranked dataset annotated as HSP20 and HSP70. HSP70 in particular is directly implicated in the thermal response of individual mosquito cohorts by Ware-Gilmore et al.,[51] while the HSP20-family homolog encodes a lethal(2) essential for life-like *(l2efl)* protein product which is additionally suggested to suppress viral entry and replication in both plants and insects.[52,53] Future studies that include multiple mosquito populations from each

developmental stage and phenotype could help to disentangle geographic variation and elucidate alleles that contribute to thermal adaptation.

While there is certainly more genetic and phenotypic variability regionally than what we measured here with two populations, these results clearly demonstrate the relevance of considering population-specific variability and local thermal adaptation in trait-based predictions. Determining the appropriate scale at which to assess variability is a challenge: regional climate classifications may be a useful starting point. The Köppen-Geiger climate classification system describes upstate NYS as a humid continental environment and downstate NYS as a humid subtropical environment.[54] Peak WNV prevalence in *Culex* spp. mosquitoes from upstate NYS was estimated to occur at a temperature 2.9°C lower than that of downstate NYS, suggesting that the population-specific R_0 models (Figure 6) based on our laboratory measures have regional relevance (Figure 1). In addition to temperature-dependent variation in transmission, numerous other factors contribute to the intensity of WNV transmission, including abundance, immune status, and phenology of hosts, and variation in viral strain.[55–59] Moisture has also been identified as a key factor influencing WNV prevalence and disease risk (reviewed in[9,60]) and in NYS both low and high soil moisture levels are associated with higher WNV transmission.[61] While it is difficult to directly measure temperature-dependent variation of R_0 in the field, variation in WNV incidence in mosquitoes is closely related to force of infection, whereas measures like human incidence of WNV neuroinvasive disease also depend on human behavior, susceptibility, and reporting processes.[11] Importantly, while Culex pools submitted for WNV surveillance testing are known to be predominately *Cx. pipiens*, they may at times include the morphologically similar *Cx. restuans*, particularly early in transmission season. *Cx. restuans* have been shown to have decreased thermal tolerance and lower optimal temperatures than *Cx. pipiens*.[12,62] Evaluating how climate variability influences this and other secondary WNV vectors is an additional consideration in refining predictive models.

While the focus of this study was to evaluate the extent to which mosquito thermal responses vary between mosquito populations, there is also well-documented temporal and geographic variability in virus genotype that could significantly affect competence.[58,59,63] In addition, increased temperatures could accelerate virus evolution and the emergence of higher fitness strains,[64] and interactions between temperature and transmission are also likely to be strain-specific.[65] Further, exposure to WNV can influence mosquito life history traits and has been shown to be associated with decreased survival in *Cx. pipiens*[66] and reduced fecundity, egg raft size and egg hatch rates in *Cx. tarsalis*.[13] Similar results have been observed with *Aedes aegypti* exposed to DENV.[67]

Irrespective of the potential impact of these additional factors, this study clearly demonstrates that utilizing population-specific empirical data to predict disease risk can inform models that more accurately predict regional differences in arbovirus transmission, both for current and future risk. While regional genetic signatures are not likely to be static, both because of continued evolution and migration, the presence of population level heterogeneity consistent with local thermal adaptation is an important consideration for projecting both patterns of transmission and appropriate interventions for vector-borne diseases with climate change.

Limitations of the study

Although mosquitoes experience a broad range of temperatures in nature, mosquito life history traits were measured at three static temperatures, limiting our capacity to accurately model WNV transmission at temperature minimum and maximum. Additionally, numerous genetically distinct mosquito populations are found throughout the region, yet for this study, only two were characterized. A broader range of populations could refine predictions in future studies.

STAR★METHODS

Detailed methods are provided in the online version of this paper and include the following:

- KEY RESOURCES TABLE
- RESOURCE AVAILABILITY
  - Lead contact
  - Materials availability
  - Data and code availability
- EXPERIMENTAL MODEL AND STUDY PARTICIPANT DETAILS
  - Mosquito rearing
- METHOD DETAILS
  - Molecular species identification
  - Mosquito development
  - Mosquito survival, feeding, and fecundity
  - Poolseq methods
  - Thermal performance curves
  - R_0 calculation
  - Mosquito surveillance and relationships to regional temperatures
  - Maps of R_0 by county
  - Plot of CMIP 6 data
- QUANTIFICATION AND STATISTICAL ANALYSIS

SUPPLEMENTAL INFORMATION

Supplemental information can be found online at https://doi.org/10.1016/j.isci.2024.109934.

ACKNOWLEDGMENTS

The authors would like to thank those who provided egg rafts for this study including Scott Campbell and Michael Santoriello at the Suffolk County Health Department and Jessica Stout at the New York State Arbovirus lab, and the maintenance staff at the Griffin laboratory for their help creating the individual holding chamber. We thank O. Elison Timm for assistance with the CMIP 6 data set. We also thank the Erie County Health Department and the New York State Bureau of Communicable Disease Control. This research was funded by NIH grant R01AI168097, NSF grant DEB-2011147 (with Fogarty International Center), NIH grant R01AI102918, NIH grant R35GM133439 and the Stanford Woods Institute for the Environment, King Center on Global Development, and Center for Innovation in Global Health.

AUTHOR CONTRIBUTIONS

Conceptualization, A.T.C.; methodology, R.L.F., M.C.L. A.C.K., D.C.P., S.D.Z, E.A.M., and A.T.C.; investigation, R.LF., M.C.L, A.C.K, D.C.P., and A.T.C.; analysis, R.L.F., M.C.L., and A.C.K.; writing – original draft, R.L.F and A.T.C; writing – review and editing, R.L.F., M.C.L., A.C.K., D.C.P., E.A.M., and A.T.C.; visualization, R.L.F., M.C.L., and A.C.K.; funding acquisition, A.T.C.; resources, E.A.M. and A.T.C.; supervision, A.T.C.

DECLARATION OF INTERESTS

The authors declare no competing interests.

Received: July 26, 2023
Revised: December 5, 2023
Accepted: May 5, 2024
Published: May 7, 2024

REFERENCES

1. Gubler, D.J. (1998). Dengue and Dengue Hemorrhagic Fever. Clin. Microbiol. Rev. *11*, 480–496. https://doi.org/10.1128/cmr.11.3.480.
2. Smithburn, K.C., Hughes, T.P., Burke, A.W., and Paul, J.H. (1940). A neurotropic virus isolated from the blood of a native of Uganda. Am. J. Trop. Med. Hyg. *20*, 471–492.
3. Farajollahi, A., Fonseca, D.M., Kramer, L.D., and Marm Kilpatrick, A. (2011). "Bird biting" mosquitoes and human disease: A review of the role of Culex pipiens complex mosquitoes in epidemiology. Infect. Genet. Evol. *11*, 1577–1585. https://doi.org/10.1016/j.meegid.2011.08.013.
4. Hayes, E.B., and Gubler, D.J. (2006). West Nile Virus: Epidemiology and Clinical Features of an Emerging Epidemic in the United States. Annu. Rev. Med. *57*, 181–194. https://doi.org/10.1146/annurev.med.57.121304.131418.
5. Bernard, K.A., Maffei, J.G., Jones, S.A., Kauffman, E.B., Ebel, G., Dupuis, A.P., Ngo, K.A., Nicholas, D.C., Young, D.M., Shi, P.-Y., et al. (2001). West Nile virus infection in birds and mosquitoes, New York State, 2000. Emerg. Infect. Dis. *7*, 679–685. https://doi.org/10.3201/eid0704.010415.
6. Kilpatrick, A.M., Kramer, L.D., Campbell, S.R., Alleyne, E.O., Dobson, A.P., and Daszak, P. (2005). West Nile Virus Risk Assessment and the Bridge Vector Paradigm. Emerg. Infect. Dis. *11*, 425–429. https://doi.org/10.3201/eid1103.040364.
7. Pachauri, R.K., Allen, M.R., Barros, V.R., Broome, J., Cramer, W., Christ, R., Church, J.A., Clarke, L., Dahe, Q., Dasgupta, P., et al. (2014). fifth Assessment Report of the Intergovernmental Panel on Climate Change. In IPCC Climate Change 2014: Synthesis Report. https://epic.awi.de/id/eprint/37530/1/IPCC_AR5_SYR_Final.pdf.
8. Rosenzweig, C., Solecki, W., DeGaetano, A., O'Grady, M., Hassol, S., and Grabhorn, P. (2011). Responding to Climate Change in New York State - Chapter 1: Climate Risks (New York State Energy Research and Development Authority (NYSERDA)). Albany, New.
9. Ciota, A.T., and Keyel, A.C. (2019). The Role of Temperature in Transmission of Zoonotic Arboviruses. Viruses *11*, 1013. https://doi.org/10.3390/v11111013.
10. Paaijmans, K.P., Heinig, R.L., Seliga, R.A., Blanford, J.I., Blanford, S., Murdock, C.C., and Thomas, M.B. (2013). Temperature variation makes ectotherms more sensitive to climate change. Global Change Biol. *19*, 2373–2380. https://doi.org/10.1111/gcb.12240.
11. Shocket, M.S., Verwillow, A.B., Numazu, M.G., Slamani, H., Cohen, J.M., El Moustaid, F., Rohr, J., Johnson, L.R., and Mordecai, E.A. (2020). Transmission of West Nile and five other temperate mosquito-borne viruses peaks at temperatures between 23°C and 26°C. Elife *9*, e58511. https://doi.org/10.7554/elife.58511.
12. Ciota, A.T., Matacchiero, A.C., Kilpatrick, A.M., and Kramer, L.D. (2014). The Effect of Temperature on Life History Traits of Culex Mosquitoes. J. Med. Entomol. *51*, 55–62. https://doi.org/10.1603/me13003.
13. Styer, L.M., Meola, M.A., and Kramer, L.D. (2007). West Nile Virus Infection Decreases Fecundity of Culex tarsalis Females. J. Med. Entomol. *44*, 1074–1085. https://doi.org/10.1603/0022-2585(2007)44[1074:wnvidf]2.0.co;2.
14. Marini, G., Poletti, P., Giacobini, M., Pugliese, A., Merler, S., and Rosà, R. (2016). The Role of Climatic and Density Dependent Factors in Shaping Mosquito Population Dynamics: The Case of Culex pipiens in Northwestern Italy. PLoS One *11*, e0154018. https://doi.org/10.1371/journal.pone.0154018.
15. Ruybal, J.E., Kramer, L.D., and Kilpatrick, A.M. (2016). Geographic variation in the response of Culex pipiens life history traits to temperature. Parasites Vectors *9*, 116. https://doi.org/10.1186/s13071-016-1402-z.
16. Dohm, D.J., O'Guinn, M.L., and Turell, M.J. (2002). Effect of Environmental Temperature on the Ability of Culex pipiens (Diptera: Culicidae) to Transmit West Nile Virus. J. Med. Entomol. *39*, 221–225. https://doi.org/10.1603/0022-2585-39.1.221.
17. Vogels, C.B.F., Fros, J.J., Göertz, G.P., Pijlman, G.P., and Koenraadt, C.J.M. (2016). Vector competence of northern European Culex pipiens biotypes and hybrids for West Nile virus is differentially affected by temperature. Parasites Vectors *9*, 393. https://doi.org/10.1186/s13071-016-1677-0.
18. Gloria-Soria, A., Armstrong, P.M., Powell, J.R., and Turner, P.E. (2017). Infection rate of Aedes aegypti mosquitoes with dengue virus depends on the interaction between temperature and mosquito genotype. Proc. Biol. Sci. *284*, 20171506. https://doi.org/10.1098/rspb.2017.1506.
19. Carrington, L.B., Seifert, S.N., Willits, N.H., Lambrechts, L., and Scott, T.W. (2013). Large Diurnal Temperature Fluctuations Negatively Influence Aedes aegypti (Diptera: Culicidae) Life-History Traits. J. Med. Entomol. *50*, 43–51. https://doi.org/10.1603/me11242.
20. Carrington, L.B., Armijos, M.V., Lambrechts, L., and Scott, T.W. (2013). Fluctuations at a

Low Mean Temperature Accelerate Dengue Virus Transmission by Aedes aegypti. PLoS Neglected Trop. Dis. *7*, e2190. https://doi.org/10.1371/journal.pntd.0002190.

21. Lambrechts, L., Paaijmans, K.P., Fansiri, T., Carrington, L.B., Kramer, L.D., Thomas, M.B., and Scott, T.W. (2011). Impact of daily temperature fluctuations on dengue virus transmission by Aedes aegypti. Proc. Natl. Acad. Sci. USA *108*, 7460–7465. https://doi.org/10.1073/pnas.1101377108.
22. Chu, V.M., Sallum, M.A.M., Moore, T.E., Lainhart, W., Schlichting, C.D., and Conn, J.E. (2019). Regional variation in life history traits and plastic responses to temperature of the major malaria vector Nyssorhynchus darlingi in Brazil. Sci. Rep. *9*, 5356. https://doi.org/10.1038/s41598-019-41651-x.
23. Mordecai, E.A., Caldwell, J.M., Grossman, M.K., Lippi, C.A., Johnson, L.R., Neira, M., Rohr, J.R., Ryan, S.J., Savage, V., Shocket, M.S., et al. (2019). Thermal biology of mosquito-borne disease. Ecol. Lett. *22*, 1690–1708. https://doi.org/10.1111/ele.13335.
24. Harrigan, R.J., Thomassen, H.A., Buermann, W., and Smith, T.B. (2014). A continental risk assessment of West Nile virus under climate change. Global Change Biol. *20*, 2417–2425. https://doi.org/10.1111/gcb.12534.
25. Ryan, S.J., Carlson, C.J., Mordecai, E.A., and Johnson, L.R. (2019). Global expansion and redistribution of Aedes-borne virus transmission risk with climate change. PLoS Neglected Trop. Dis. *13*, e0007213. https://doi.org/10.1371/journal.pntd.0007213.
26. Sargent, K., Mollard, J., Henley, S.F., and Bollasina, M.A. (2022). Predicting Transmission Suitability of Mosquito-Borne Diseases under Climate Change to Underpin Decision Making. Int. J. Environ. Res. Public Health *19*, 13656. https://doi.org/10.3390/ijerph192013656.
27. Wimberly, M.C., Davis, J.K., Hildreth, M.B., and Clayton, J.L. (2022). Integrated Forecasts Based on Public Health Surveillance and Meteorological Data Predict West Nile Virus in a High-Risk Region of North America. Environ. Health Perspect. *130*, 087006. https://doi.org/10.1289/ehp10287.
28. Wimberly, M.C., and Davis, J.K. (2019). GRIDMET_downloader.js. (1.1) [Java Script].
29. Abatzoglou, J.T. (2013). Development of gridded surface meteorological data for ecological applications and modelling. Int. J. Climatol. *33*, 121–131. https://doi.org/10.1002/joc.3413.
30. Harbach, R.E., Harrison, B.A., and Gad, A.M. (1984). Culex (Culex) molestus Forskal (Diptera: Culicidae): neotype designation, description, variation, and taxonomic status. Proc. Entomol. Soc. Wash. *86*, 521–542.
31. Harbach, R.E., Dahl, C., and White, G.B. (1985). Culex (Culex) pipiens Linnaeus (Diptera, Culicidae)-concepts, type designations, and description. Proc. Entomol. Soc. Wash. *1*, 1–24.
32. Bahnck, C.M., and Fonseca, D.M. (2006). Rapid assay to identify the two genetic forms of Culex (Culex) pipiens L. (Diptera: Culicidae) and hybrid populations. Am. J. Trop. Med. Hyg. *75*, 251–255.
33. Mordecai, E.A., Cohen, J.M., Evans, M.V., Gudapati, P., Johnson, L.R., Lippi, C.A., Miazgowicz, K., Murdock, C.C., Rohr, J.R., Ryan, S.J., et al. (2017). Detecting the impact of temperature on transmission of Zika, dengue, and chikungunya using mechanistic models. PLoS Neglected Trop. Dis. *11*, e0005568. https://doi.org/10.1371/journal.pntd.0005568.
34. Shocket, M.S., Ryan, S.J., and Mordecai, E.A. (2018). Temperature explains broad patterns of Ross River virus transmission. Elife *7*, e37762. https://doi.org/10.7554/elife.37762.
35. Tesla, B., Demakovsky, L.R., Mordecai, E.A., Ryan, S.J., Bonds, M.H., Ngonghala, C.N., Brindley, M.A., and Murdock, C.C. (2018). Temperature drives Zika virus transmission: evidence from empirical and mathematical models. Proc. Biol. Sci. *285*, 20180795. https://doi.org/10.1098/rspb.2018.0795.
36. Keyel, A.C., Raghavendra, A., Ciota, A.T., and Elison Timm, O. (2021). West Nile virus is predicted to be more geographically widespread in New York State and Connecticut under future climate change. Global Change Biol. *27*, 5430–5445. https://doi.org/10.1111/gcb.15842.
37. Paull, S.H., Horton, D.E., Ashfaq, M., Rastogi, D., Kramer, L.D., Diffenbaugh, N.S., and Kilpatrick, A.M. (2017). Drought and immunity determine the intensity of West Nile virus epidemics and climate change impacts. Proc. Biol. Sci. *284*, 20162078. https://doi.org/10.1098/rspb.2016.2078.
38. Spanoudis, C.G., Andreadis, S.S., Tsaknis, N.K., Petrou, A.P., Gkeka, C.D., and SavopoulouSoultani, M. (2019). Effect of Temperature on Biological Parameters of the West Nile Virus Vector Culex pipiens form molestus (Diptera: Culicidae) in Greece: Constant vs Fluctuating Temperatures. J. Med. Entomol. *56*, 641–650. https://doi.org/10.1093/jme/tjy224.
39. Muttis, E., Balsalobre, A., Chuchuy, A., Mangudo, C., Ciota, A.T., Kramer, L.D., and Micieli, M.V. (2018). Factors Related to Aedes aegypti (Diptera: Culicidae) Populations and Temperature Determine Differences on Life-History Traits With Regional Implications in Disease Transmission. J. Med. Entomol. *55*, 1105–1112. https://doi.org/10.1093/jme/tjy057.
40. Vorhees, A.S., Gray, E.M., and Bradley, T.J. (2013). Thermal Resistance and Performance Correlate with Climate in Populations of a Widespread Mosquito. Physiol. Biochem. Zool. *86*, 73–81. https://doi.org/10.1086/668851.
41. Dodson, B.L., Kramer, L.D., and Rasgon, J.L. (2012). Effects of larval rearing temperature on immature development and West Nile virus vector competence of Culex tarsalis. Parasites Vectors *5*, 199. https://doi.org/10.1186/1756-3305-5-199.
42. Reisen, W.K. (1995). Effect of Temperature on Culex tarsalis (Diptera: Culicidae) from the Coachella and San Joaquin Valleys of California. J. Med. Entomol. *32*, 636–645. https://doi.org/10.1093/jmedent/32.5.636.
43. Mogi, M. (1992). Temperature and Photoperiod Effects on Larval and Ovarian Development of New Zealand Strains of Culex quinquefasciatus (Diptera: Culicidae). Ann. Entomol. Soc. Am. *85*, 58–66. https://doi.org/10.1093/aesa/85.1.58.
44. Couper, L.I., Farner, J.E., Caldwell, J.M., Childs, M.L., Harris, M.J., Kirk, D.G., Nova, N., Shocket, M., Skinner, E.B., Uricchio, L.H., et al. (2021). How will mosquitoes adapt to climate warming? Elife *10*, e69630. https://doi.org/10.7554/elife.69630.
45. Vinogradova, E.B. (2000). Culex pipiens pipiens mosquitoes: taxonomy, distribution, ecology, physiology, genetics, applied importance and control (Pensoft).
46. Kehoe, K., Noels, H., Theelen, W., De Hert, E., Xu, S., Verrijken, A., Arnould, T., Fransen, E., Hermans, N., Lambeir, A.-M., et al. (2018). Prolyl carboxypeptidase activity in the circulation and its correlation with body weight and adipose tissue in lean and obese subjects. PLoS One *13*, e0197603. https://doi.org/10.1371/journal.pone.0197603.
47. Zhu, F., Moural, T.W., Shah, K., and Palli, S.R. (2013). Integrated analysis of cytochrome P450 gene superfamily in the red flour beetle, Tribolium castaneum. BMC Genom. *14*, 174. https://doi.org/10.1186/1471-2164-14-174.
48. Wang, J., Fan, H., Wang, P., and Liu, Y.-H. (2019). Expression Analysis Reveals the Association of Several Genes with Pupal Diapause in Bactrocera minax (Diptera: Tephritidae). Insects *10*, 169. https://doi.org/10.3390/insects10060169.
49. Zhang, Y., Liu, S., Meyer, M.D., Liao, Z., Zhao, Y., Virgilio, M., Feng, S., Qin, Y., Singh, S., Wee, S.L., et al. (2022). Genomes of the cosmopolitan fruit pest Bactrocera dorsalis (Diptera: Tephritidae) reveal its global invasion history and thermal adaptation. J. Adv. Res. *53*, 61–74. https://doi.org/10.1016/j.jare.2022.12.012.
50. Lv, W.-X., Cheng, P., Lei, J.-J., Peng, H., Zang, C.-H., Lou, Z.-W., Liu, H.-M., Guo, X.-X., Wang, H.-Y., Wang, H.-F., et al. (2023). Interactions between the gut microcommunity and transcriptome of Culex pipiens pallens under low-temperature stress. Parasites Vectors *16*, 12. https://doi.org/10.1186/s13071-022-05643-7.
51. Ware-Gilmore, F., Novelo, M., Sgrò, C.M., Hall, M.D., and McGraw, E.A. (2023). Assessing the role of family level variation and heat shock gene expression in the thermal stress response of the mosquito Aedes aegypti. Philos. Trans. R. Soc. Lond. B Biol. Sci. *378*, 20220011. https://doi.org/10.1098/rstb.2022.0011.
52. Li, J., Xiang, C.-Y., Yang, J., Chen, J.-P., and Zhang, H.-M. (2015). Interaction of HSP20 with a viral RdRp changes its sub-cellular localization and distribution pattern in plants. Sci. Rep. *5*, 14016. https://doi.org/10.1038/srep14016.
53. Runtuwene, L.R., Kawashima, S., Pijoh, V.D., Tuda, J.S.B., Hayashida, K., Yamagishi, J., Sugimoto, C., Nishiyama, S., Sasaki, M., Orba, Y., et al. (2020). The Lethal(2)-Essential-for-Life [L(2)EFL] Gene Family Modulates Dengue Virus Infection in Aedes aegypti. Int. J. Mol. Sci. *21*, 7520. https://doi.org/10.3390/ijms21207520.
54. Beck, H.E., Zimmermann, N.E., McVicar, T.R., Vergopolan, N., Berg, A., and Wood, E.F. (2018). Present and future Köppen-Geiger climate classification maps at 1-km resolution. Sci. Data *5*, 180214. https://doi.org/10.1038/sdata.2018.214.
55. Kain, M.P., and Bolker, B.M. (2019). Predicting West Nile virus transmission in North American bird communities using phylogenetic mixed effects models and eBird citizen science data. Parasites Vectors *12*, 395. https://doi.org/10.1186/s13071-019-3656-8.
56. Kilpatrick, A.M., Daszak, P., Jones, M.J., Marra, P.P., and Kramer, L.D. (2006). Host heterogeneity dominates West Nile virus transmission. Proc. Biol. Sci. *273*, 2327–2333. https://doi.org/10.1098/rspb.2006.3575.
57. Kramer, L.D., Ciota, A.T., and Kilpatrick, A.M. (2019). Introduction, Spread, and Establishment of West Nile Virus in the Americas. J. Med. Entomol. *56*, 1448–1455. https://doi.org/10.1093/jme/tjz151.

58. Moudy, R.M., Meola, M.A., Morin, L.-L.L., Ebel, G.D., and Kramer, L.D. (2007). A newly emergent genotype of West Nile virus is transmitted earlier and more efficiently by Culex mosquitoes. Am. J. Trop. Med. Hyg. *77*, 365–370.
59. Bialosuknia, S.M., Dupuis, A.P., Zink, S.D., Koetzner, C.A., Maffei, J.G., Owen, J.C., Landwerlen, H., Kramer, L.D., and Ciota, A.T. (2022). Adaptive evolution of West Nile virus facilitated increased transmissibility and prevalence in New York State: Adaptive evolution of West Nile virus in New York State. Emerg. Microb. Infect. 1–32. https://doi.org/10.1080/22221751.2022.2056521.
60. Fay, R.L., Keyel, A.C., and Ciota, A.T. (2022). West Nile virus and climate change. Adv. Virus Res. 147–193. https://doi.org/10.1016/bs.aivir.2022.08.002.
61. Keyel, A.C., Elison Timm, O., Backenson, P.B., Prussing, C., Quinones, S., McDonough, K.A., Vuille, M., Conn, J.E., Armstrong, P.M., Andreadis, T.G., and Kramer, L.D. (2019). Seasonal temperatures and hydrological conditions improve the prediction of West Nile virus infection rates in Culex mosquitoes and human case counts in New York and Connecticut. PLoS One *14*, e0217854. https://doi.org/10.1371/journal.pone.0217854.
62. Andreadis, T.G., Anderson, J.F., and Vossbrinck, C.R. (2001). Mosquito surveillance for West Nile virus in Connecticut, 2000: isolation from Culex pipiens, Cx. restuans, Cx. salinarius, and Culiseta melanura. Emerg. Infect. Dis. *7*, 670–674. https://doi.org/10.3201/eid0704.010413.
63. Bialosuknia, S.M., Tan, Y., Zink, S.D., Koetzner, C.A., Maffei, J.G., Halpin, R.A., Muller, E., Novatny, M., Shilts, M., Fedorova, N.B., et al. (2019). Evolutionary dynamics and molecular epidemiology of West Nile virus in New York State: 1999–2015. Virus Evol. *5*, vez020. https://doi.org/10.1093/ve/vez020.
64. Fay, R.L., Ngo, K.A., Kuo, L., Willsey, G.G., Kramer, L.D., and Ciota, A.T. (2021). Experimental Evolution of West Nile Virus at Higher Temperatures Facilitates Broad Adaptation and Increased Genetic Diversity. Viruses *13*, 1889. https://doi.org/10.3390/v13101889.
65. Kilpatrick, A.M., Meola, M.A., Moudy, R.M., and Kramer, L.D. (2008). Temperature, Viral Genetics, and the Transmission of West Nile Virus by Culex pipiens Mosquitoes. PLoS Pathog. *4*, e1000092. https://doi.org/10.1371/journal.ppat.1000092.
66. Ciota, A.T., Styer, L.M., Meola, M.A., and Kramer, L.D. (2011). The costs of infection and resistance as determinants of West Nile virus susceptibility in Culex mosquitoes. BMC Ecol. *11*, 23. https://doi.org/10.1186/1472-6785-11-23.
67. Maciel-de-Freitas, R., Koella, J.C., and Lourenço-de-Oliveira, R. (2011). Lower survival rate, longevity and fecundity of Aedes aegypti (Diptera: Culicidae) females orally challenged with dengue virus serotype 2. Trans. Roy. Soc. Trop. Med. Hyg. *105*, 452–458. https://doi.org/10.1016/j.trstmh.2011.05.006.
68. Cheng, P., Zhang, Q., Zhang, X., Le, Q., Gong, M., Zhang, Z., and Zhang, R. (2021). A drat genome assembly of Culex pipiens pallens (Diptera: Culicidae) using PacBio sequencing. Genome Biol. Evol. *13*, evab005. https://doi.org/10.1093/gbe/evab005.
69. Plummer, M. (2003). JAGS: a program for analysis of bayesian graphical models using gibbs sampling. In Proceedings of the 3rd International Workshop on Distributed Statistical Computing, pp. 1–10.
70. Curtis, S.M., Goldin, I., and Evangelou, E. (2018). Mcmcplots.
71. Eyring, V., Bony, S., Meehl, G.A., Senior, C.A., Stevens, B., Stouffer, R.J., and Taylor, K.E. (2016). Overview of the Coupled Model Intercomparison Project Phase 6 (CMIP6) experimental design and organization. Geosci. Model Dev. *9*, 1937–1958. https://doi.org/10.5194/gmd-9-1937-2016.
72. Dodson, B.L., Kramer, L.D., and Rasgon, J.L. (2011). Larval Nutritional Stress Does Not Affect Vector Competence for West Nile Virus (WNV) in Culex tarsalis. Vector Borne Zoonot Dis. *11*, 1493–1497. https://doi.org/10.1089/vbz.2011.0662.
73. Pilitt, D.R., and Jones, J.C. (1972). A Qualitative Method for Estimating the Degree of Engorgement of Aedes Aegypti Adults1. J. Med. Entomol. *9*, 334–337. https://doi.org/10.1093/jmedent/9.4.334.
74. Micheletti, S.J., and Narum, S.R. (2018). Utility of pooled sequencing for association mapping in nonmodel organisms. Mol. Ecol. Resour. *18*, 825–837. https://doi.org/10.1111/1755-0998.12784.
75. Kofler, R., Pandey, R.V., and Schlötterer, C. (2011). PoPoolation2: identifying differentiation between populations using sequencing of pooled DNA samples (Pool-Seq). Bioinformatics *27*, 3435–3436. https://doi.org/10.1093/bioinformatics/btr589.
76. Wright, R.M., Aglyamova, G.V., Meyer, E., and Matz, M.V. (2015). Gene expression associated with white syndromes in a reef building coral, Acropora hyacinthus. BMC Genom. *16*, 371. https://doi.org/10.1186/s12864-015-1540-2.
77. Su, Y.-S., and Yajima, M. (2009). 2jags: A Package for Running Jags from R. 0.6-1.
78. Zink, S.D., Jones, S.A., Maffei, J.G., and Kramer, L.D. (2013). Quadraplex qRT-PCR assay for the simultaneous detection of Eastern equine encephalitis virus and West Nile virus. Diagn. Microbiol. Infect. Dis. *77*, 129–132. https://doi.org/10.1016/j.diagmicrobio.2013.06.019.
79. Team, R.C. (2020). R: A Language and Environment for Statistical Computing.
80. Hijmans, R.J. (2023). Terra: Spatial Data Analysis. R package version 1.6-53.
81. Made with Natural Earth. Free vector and raster map data. https://www.naturalearthdata.com/downloads/10m-cultural-vectors/.
82. 2021, United States Census Bureau (2021). TIGER/Line Shapefiles.
83. Keyel, A.C. (2023). Patterns of West Nile Virus in the Northeastern United States Using Negative Binomial and Mechanistic Trait-Based Models. Geohealth *7*, e2022GH000747. https://doi.org/10.1029/2022gh000747.
84. Ayompe, L.M., Davis, S.J., and Egoh, B.N. (2020). Trends and drivers of African fossil fuel CO2 emissions 19902017. Environ. Res. Lett. *15*, 124039. https://doi.org/10.1088/1748-9326/abc64f.

STAR★METHODS

KEY RESOURCES TABLE

REAGENT or RESOURCE	SOURCE	IDENTIFIER
Critical commercial assays		
Biosciences qScript XLT One-Step qRT-PCR Toughmix kit	VWR	Cat# 76047-136
MagMAX™ Wash Solution 2 Concentrate	Thermo Fisher	Cat# AM8640
DNA Binding Beads for MagMAX™ DNA Multi-Sample Ultra Kit	Thermo Fisher	Cat# A25562
MagMAX™ Wash Solution 1 Concentrate	Thermo Fisher	Cat# AM8504
MagMAX™ Lysis/Binding Solution Concentrate	Thermo Fisher	Cat# AM8500
Carrier RNA	Thermo Fisher	Cat# 4382878
Qiagen DNeasy-96 plate extraction kit	Fisher Scientific	Cat#6 9581
Qubit dsDNA high-sensitivity kit	Fisher Scientific	Cat# Q32851
Illumina DNA Sample prep kit	Illumina	Cat# 20060059
Deposited data		
Genome assembly of *Culex pipiens pallens*	Cheng et al. 2021[68]	https://figshare.com/articles/figure/Genome_assembly_of_Culex_pipiens_pallens/13324319/1
Culex pipiens upstate genome	NCBI	https://www.ncbi.nlm.nih.gov/bioproject/PRJNA1028265/
Culex pipiens downstate genome	NCBI	https://www.ncbi.nlm.nih.gov/bioproject/PRJNA1028265/
Culex pipiens life history trait data	GitHub	https://github.com/mcruzloya/NY2pop
Experimental models: Organisms/strains		
Culex pipiens downstate	Yaphank, NY	N/A
Culex pipiens upstate	Albany, NY	N/A
Oligonucleotides		
Culex restuans reverse primer ACATTATTTGAGGCCTACATGG	Integrated DNA Technologies	*Culex restuans*_R
Culex restuans forward primer TGGGCGACGATGTAACC	Integrated DNA Technologies	*Culex restuans*_F
Culex pipiens forward primer CGCCGATGT AGCATCTC	Integrated DNA Technologies	*Culex pipiens*_F
Culex restuans Probe /5Cy3/TAACCTCTCACACTCC TGCGTTGAC/3IAbRQSp/)	Integrated DNA Technologies	*Culex restuans* Probe
Culex pipiens probe (/56-FAM/AGCAGCGAA/ZEN/CGACA AGCGATAT/3IABkFQ/	Integrated DNA Technologies	*Culex pipiens* probe
Software and algorithms		
R package R2jags	Plummer et al. 2003[69]	https://cran.r-project.org/web/packages/R2jags/index.html
Mcmc plots	Curtis et al. 2018[70]	https://cran.r-project.org/web/packages/mcmcplots/index.html
CMIP6	Eyring et al. 2016[71]	https://doi.org/10.5194/gmd-9-1937-2016
GRIDMET	Abatzoglou, 2013[29]	https://doi.org/10.1002/joc.3413
Other		
Defibrinated chicken blood	Colorado Serum Company	Cat# 31143

RESOURCE AVAILABILITY

Lead contact

Further information and requests for resources should be directed to and will be fulfilled by the lead contact, Alexander Ciota (alexander.ciota@health.ny.gov).

Materials availability

This study did not generate new unique reagents.

Data and code availability

- All data sets reported in this work are publicly available on Github https://github.com/mcruzloya/NY2pop and NCBI BioProject PRJNA1028265.
- Code is available on Github https://github.com/mcruzloya/NY2pop and https://github.com/z0on/GO_MWU.
- Any additional information required to reanalyze the data reported in this paper is available from the lead contact upon request.

EXPERIMENTAL MODEL AND STUDY PARTICIPANT DETAILS

Mosquito rearing

Egg rafts of the downstate NYS *Culex pipiens* population were originally collected in Yaphank, NY in 2020 (40.82987 °N, 72.91851 °W). Egg rafts of the upstate NYS *Culex pipiens* population was originally collected in Albany, NY in 2021 (42.65379 °N, 73.76233 °W). Field populations were maintained at the NYS Arbovirus Laboratory in an 18-24 inch^2 cage in an incubator at constant temperature of 25°C with a relative humidity of 45-85%, photoperiod of 16:8 (L:D) and a grow light at dawn and dusk. Speciation was initially performed by morphological identification of larvae and adults. Some lab amplification was required to attain sufficient sample sizes. The 3rd generation (F3) of the downstate population and the 2nd generation (F2) of the of the upstate population were used for this study.

METHOD DETAILS

Molecular species identification

Individual mosquitoes were homogenized in 500 μL of mosquito diluent containing 20% fetal bovine serum, 50 μg of streptomycin per mL, 50 μL of penicillin, and 2.5 μg of amphotericin B per mL in phosphate-buffered saline, in a Retsch Mixer Mill set to 24 cycles/s for 2 min. The tubes were then centrifuged for 4 min at 12,000 rpm. Extraction plates were prepared on a Tecan Evo 150 liquid handler and 50 μL of homogenates were used to extract RNA on a Magmax 96 Express using a MagMax viral isolation kit (Thermo Fisher, Waltham, MA). A total of 90 μL of homogenized sample RNA was eluted. Real-time RT–PCR assay was performed by using a universal reverse primer and unique forward primers and probes, to allow for differentiation between *Culex restuans* and *Culex pipiens*. Primers and probes were designed to target the 5.8S rRNA of *Culex restuans* and *Culex pipiens* genome, *Culex restuans*_R (ACATTATTTGAGGCCTACATGG), *Culex restuans*_F (TGGGCGACGATGTAACC) and *Culex pipiens*_F (CGCCGATGT AGCATCTC) (Integrated DNA Technologies, Coralville, IA). Probes utilized include *Culex restuans* Probe (/5Cy3/TAACCTCTCACACTCCTGCGTTGAC/3IAbRQSp/) and *Culex pipiens* probe (/56-FAM/AGCAGCGAA/ZEN/CGACAAGCGATAT/3IABkFQ/) (Integrated DNA Technologies, Coralville, IA). Assays were performed on the Applied Biosystems QuantStudio 5 Real-Time PCR System using Quanta Biosciences qScript XLT One-Step qRT-PCR Toughmix kit (VWR, Radnor, PA). Thermal cycling consisted of 50°C for 3 min for RT, 95°C for 10 min, and 40 cycles of 95°C for 3 s and 60°C for 30 min. A sample was considered positive if the CT value was less than 40 for either primer set.

Mosquito development

After hatching, 100 larvae per population were counted and equally distributed into two transparent 11 x 6.6 x 2.7 inch plastic containers with 250 mL of filtered water using a transfer pipette. Larvae were then placed in incubators and subjected to photoperiod of 16:8 (L:D) h and grow light, under constant temperatures (22, 25, or 28°C). These temperatures were shown to mimic regional temperatures relevant to these unique populations and a predicted future temperature. Water dishes were placed inside the chambers to maintain humidity and temperatures were monitored and recorded daily. Larvae were fed ground koi food every other day in increasing quantities as follows: 60 mg first and second instar, 80 mg third instar, and 100 mg fourth instar. Developing larvae were monitored daily for mortality, and dead larvae were counted, recorded, and discarded. Daily pupation was also recorded, and pupae were placed using a transfer pipette in distilled water in emergence jars in preparation for eclosion.

Mosquito survival, feeding, and fecundity

Newly emergent mosquitoes were sexed and counted. Adults were grouped and housed in gallon size cardboard containers via aspirator as they emerged and held for 1 day after last emergence to allow for mating. Females were knocked down using CO_2 and were placed in individual 50 mL conical tubes placed in Styrofoam rack, with a hole in the top of the conical covered in mesh, a hole in bottom of the conical to allow addition of water for laying, and a dental dam around bottom of the conical to hold the tube in place. Cotton pads soaked in 10%

sucrose *ad libitum* were placed on top of the conicals. The number of emerged female adults varied at each temperature, of the upstate population 48 adults were individually housed at 22°C, 50 at 25°C, 17 at 28°C, of the downstate population 50 were individually housed at 22°C, 49 at 25°C and 50 at 28°C. Survival of all groups was monitored and recorded daily. Wings from 20 adults per group per temperature were removed and placed on slides with double-sided tape and were subsequently measured from the alular notch to the distal margin, excluding the fringe using a Keyence All-in-One Fluorescence Microscope BZ-X800E to estimate mosquito size.[72] Mosquitoes were starved overnight for 12- 24 h and offered 200-ul defibrinated chicken blood (Colorado Serum Company, Denver, CO) with 2.5% sucrose via absorbent pad for 2-h every 4-5 days. Mosquitoes were monitored for feeding activity during this period, and the degree of engorgement was recorded (1, blood first appears in abdomen, no abdominal distention; 2, slight abdominal distension, no pleural membrane observed; 3, pleural membrane observed; and 4, fully distended abdomen).[73] The bottom of conicals were checked daily for eggs; when eggs were observed in a conical, the egg raft was transferred using a wooden stick to a petri dish. Digital pictures were taken of each egg raft under a research stereo microscope by using a Nikon SMZ18 and ACCU-SCOPE AU-600-HD, Excelis HD Camera with C-mount adapter. The number of eggs in each egg raft was determined by counting individual eggs in the digital pictures using CaptaVision. Statistical analyses were performed using GraphPad Prism 9.3.1.

Poolseq methods

Fifty individual downstate and 28 individual upstate F2 female *Cx. pipiens* mosquitoes were homogenized in 96-well plates and extracted using the Qiagen DNeasy-96 plate extraction kit (Qiagen, Hilden, Germany) per manufacturer protocol and eluted in 80uL of elution buffer. Each elution was quantified using a Qubit dsDNA high-sensitivity kit (Thermo Fisher, Waltham, MA) and equal amounts of DNA from each individual were pooled by population. Two Illumina sequencing libraries were created (one per pool/population) using the Illumina DNA Sample prep kit (Illumina Inc, San Diego, CA) and pooled in equimolar concentrations prior to sequencing on an Illumina HiSeq 2500 instrument in a 150x150bp paired-end configuration.

The reads were trimmed of adapter and low-quality bases, mapped to the *Culex pipiens pallens* reference genome,[68] and between-population allele frequencies for identified SNPs at sites with a minimum coverage of 10x and maximum of 70x were generated using the PoolParty pipeline[74] which additionally relies on Popoolation2[75] for calculation. Significance of each SNP was assessed with a Fisher's exact test ($p < 0.05$), and significant SNPs per bp (i.e., normalized by gene length) were calculated for the 16,681 annotated *Cx. pipiens pallens* genes retrieved from the[68] supplemental data repository (https://figshare.com/articles/figure/Genome_assembly_of_Culex_pipiens_pallens/13324319/1) with an average minimum mapping coverage $\geq$ 10x. A single gene isoform was reported for each structure in this dataset. The 95th percentile (top 5%) of genes sorted by descending significant SNPs per bp of gene CDS sequence were used as a test set moving forward to assess GO enrichment via Mann-Whitney U-test (using binary [test/reference set] data as opposed continuous measures) with R using code applied in[76] and made available at https://github.com/z0on/GO_MWU. The short-read Illumina sequence data for upstate and downstate Culex pipiens populations can be accessed via NCBI BioProject PRJNA1028265.

Thermal performance curves

A Bayesian approach was used to fit thermal performance curves (TPCs) to each measured trait (lifespan, fecundity, biting rate, mosquito development rate, proportion of larvae surviving to adulthood, and proportion ovipositing). A separate TPC was fit for each trait to the upstate and downstate NYS *Culex pipiens* populations. We followed a similar approach as in[11] choosing between linear, quadratic, or Briére functions, depending on the trait. Except for biting rate, which was better fit by a quadratic function (see Appendix), the final functional forms chosen for each trait were identical to those used in Shocket et al. To constrain the fitted thermal curves to reasonable thermal limits, informative priors were used on model parameters based on previous fits to *Culex pipiens* data.[11] To facilitate comparisons between the populations, the same statistical model (with identical prior distributions) was always used for the upstate and downstate mosquito populations. For details on the specific model used for each trait (including a full justification of the prior distributions) see Appendix. To evaluate the robustness of our results to the choice of prior distributions, we performed a prior sensitivity analysis in which the prior distributions were made less informative or more informative than those in the main text. Details of this sensitivity analysis and the estimated parameters under these alternate choices of priors are available in the Appendix.

Models were fit using Markov Chain Monte Carlo (MCMC) with the r2jags R package,[77] an interface for the JAGS (Just Another Gibbs Sampler) program.[69] Three independent MCMC chains were run for 300,000 iterations, discarding the first 50,000 iterations as burn-in.[70] The resulting MCMC chains were thinned, saving every eight iterations. Chain convergence was monitored both by visual inspection of trace plots and density plots of the individual chains and by ensuring the potential scale reduction factor $\widehat{R} < 1.01$ for all parameters. For traits in which the number of effective samples n_{eff} for some model parameters was substantially lower than 10,000, the number of MCMC iterations was increased to 1,000,000 with a 50,000 burn-in. This ensured $n_{eff} > 10000$ for almost all parameters (and $n_{eff} > 9000$ for all parameters). A summary of the posterior distribution (mean, 95% credible interval [CI], $\widehat{R}$, n_{eff}) for all model parameters corresponding to the TPC fit for each trait is available in the Appendix. Optimal temperatures were calculated analytically using the posterior samples of the model parameters (for details on the mathematical expressions used and their derivation from the corresponding TPC model equation, see Appendix). Code utilized during this study can be found at https://github.com/mcruzloya/NY2pop.

R_0 calculation

The temperature dependence of the basic reproductive number R_0 for WNV in both mosquito populations was estimated with the relative R_0 approach, as in Shocket et al. 2020.[11] Due to the units in the lab measurements in this work, the model was parameterized in terms of eggs per raft, proportion ovipositing and egg viability, as follows:

$$\text{relative } R_0(T) = \sqrt{\frac{a^3(T)bc(T)e^{-\frac{\mu(T)}{\text{PDR}(T)}}\text{ER}(T)p_O(T)\text{EV}(T)p_{LA}(T)\text{MDR}(T)}{\mu^3(T)}}$$

The MCMC posterior draws from the thermal performance curve fits were used to calculate posterior draws for relative $R_0(T)$ as a function of temperature. For traits that were not measured for the mosquito populations in this work (vector competence $bc(T)$, pathogen development rate PDR(T) and egg viability EV(T)), we used posterior draws from previously obtained TPC fits to *Culex pipiens* data in.[11] Thus, our approach assumes that these traits are identical in the upstate and downstate mosquito populations, which may underestimate the differences in R_0 between the populations. For more details about the R_0 calculation, see Appendix and https://github.com/mcruzloya/NY2pop.

Mosquito surveillance and relationships to regional temperatures

Data was compiled from trapping and testing completed in Suffolk County (downstate) and Erie County (upstate). Although Erie County is located in Western NYS, distant from the origin of the upstate mosquito population utilized for experiments, it is the only upstate county that regularly submits high numbers of *Culex* spp. for weekly WNV testing. Further, temperature profiles during transmission season are similar between Erie and Albany Counties. Culex mosquitoes were collected in Centers for Disease Control (CDC) light traps by NYS county health departments and pools are submitted to the NYS Arbovirus Laboratory for processing and testing. Pools consisted of up to 60 females in 1 mL mosquito diluent [MD, 20% heat-inactivated fetal bovine serum (FBS) in Dulbecco's phosphate-buffered saline (PBS) plus 50 μg/mL penicillin/streptomycin, 50 μg/mL gentamicin, and 2.5 μg/mL Fungizone] with 1 steel bead (Daisy Outdoor Products, Rogers, AR). Processing of samples consisted of 30 s of homogenization at 24 Hz in a Mixer Mill MM301 (Retsch, Newtown, PA), followed by centrifugation at 6000 rcf for 5 min. WNV-positive pools were identified by quantitative real-time reverse transcription polymerase chain reaction (qRT-PCR).[78] WNV prevalence was determined using maximum likelihood estimation (MLE) based on mosquito surveillance pool sizes using an Excel Add-In (https://www.cdc.gov/westnile/resourcepages/mosqSurvSoft.html). Weekly temperatures during WNV transmission season (7/17-10/2) were derived from GRIDMET[29] using a downloader tool[28] and plotted against WNV prevalence. A 2-week lag was used to better show the effects of temperature on WNV transmission.

Maps of R_0 by county

R_0 was estimated by county for the present day and for one to three degrees of future warming. Temperature data were downloaded using the data downloader tool[28] from the Gridmet Dataset[29] on Google Earth Engine. Data were downloaded by county for 2021 and averaged for the months of July and August to represent relative risk during the peak mosquito season. Relative risk was calculated separately for upstate and downstate counties. Downstate was defined as all counties south of Orange and Putnam counties, including Orange and Putnam counties, and included New York City and Long Island. Upstate counties used the relative risk from the temperature-trait models for the Albany population of mosquitoes, while downstate used relative risk from the Suffolk mosquito population. Temperatures were averaged in R,[79] and maps were created using the terra package in R[80] using a Natural Earth counties base map.[81] Figure 1 was created in ArcGIS 10.6 (ESRI, Redlands, CA), and the inset used US Census 2021 state boundaries.[82] Confidence intervals correspond to those from the relative R_0 modeling, merged to county by temperature. Future warming was estimated in this case by simply adding the warming to each county. As a consequence, this does not match up to any IPCC scenario, as different counties are expected to warm at slightly different rates but does provide a climate-scenario-independent means of assessing potential risk for a set amount of warming.[83]

Plot of CMIP 6 data

The 6th phase of the Coupled Model Intercomparison Project (CMIP 6) groups data into several scenarios.[71] Of relevance to this paper are the historical scenario, and the shared socioeconomic pathway (SSP) scenarios 1, 2, 5. Scenario 1 corresponds to Representative Concentration Pathway (RCP) 2.6 from prior model comparison products and represents a best-case scenario of immediate reductions in CO_2-equivalent emissions. Scenario 2 corresponds to RCP 4.5 and represents a scenario with gradual emission reductions over time. Scenario 5 corresponds to a scenario with no greenhouse gas emission reductions. The IPCC does not consider a scenario in which CO_2 emissions continue to increase (e.g., through increased fossil fuel use by developing nations[84]) so there may be potential future warming beyond what is modeled here.

Monthly temperature data were downloaded from the Google Cloud CMIP6 Public Data repository for projections from 2015 - 2100 using jupyter scripts developed by Oliver Elison Timm. Data were downloaded for the entire state of New York based on a bounding box based on latitude (40.47 – 45.02 °N) and longitude (71.83 – 79.83 °W) and averaged to give a single temperature estimate for the entire region. The CMIP 6 data base was searched for model runs with historical, SSP 1, SSP 2 and SSP 5 model runs (40 models for historical and SSP 1, 39 models for SSPs 2 and 5). The temperature lines represent the median temperature across all models for the scenario. In the right panel, the estimated

R_0's for each population were applied to the statewide future estimated temperature. As a consequence, county-specific trajectories may vary, and future research could apply a bias correction or utilize statistically downscaled data to get future estimates by county for county-specific planning purposes.

QUANTIFICATION AND STATISTICAL ANALYSIS

Statistical analyses performed include Two-Way ANOVA and chi-squared tests. Except for the thermal performance curve and relative R0 estimation (approach described above), all statistics were performed using GraphPad Prism 9.3.1. Statistical details can be found in the figure legends and results.